1

Thermodynamic Cycles

1.1 Introduction to Thermodynamic Cycles

The concept of a thermodynamic cycle is based on depicting thermodynamic processes which involve the transfer heat and work. This is achieved by altering temperature, pressure, as well as other state variables; the cycle ultimately returning to its initial state. The fundamental basis of these cycles is the first law of thermodynamics which states that 'energy cannot be created nor destroyed but only converted from one form to another'.

As shown in Figure 1.1, thermodynamic cycles are split into two primary classes – refrigeration cycles (also known as heat pump cycles) and power cycles such as the combustion engine cycle.

Cycles which transfer heat from low temperature to high temperature are classified as heat pump cycles, whereas cycles that convert heat input into mechanical work are designated as power cycles. And so, not inappropriately, thermodynamic power cycles provide the foundation for the operation of a heat engine. Power cycles are then further divided into groups depending on the type of heat engine. For cycles modelling internal combustion engines the groups are the Otto, Diesel, and Brayton cycles and for external combustion engines, they are the Rankine, Organic Rankine, and Kalina cycles.

1.2 Rankine Cycle

1.2.1 Introduction

The Rankine cycle is a closed thermodynamic cycle that converts thermal energy into mechanical energy and is based on the fundamentals of the Carnot cycle proposed by the French physicist Nicolas Léonard Sadi Carnot in 1824. The Rankine cycle was proposed by the Scottish physicist William John Macquorn Rankine in 1865, and contrary to Carnot cycle – which is only a theoretical cycle – the Rankine cycle has many applications, several of which will be discussed further within this section.

The main application of the Rankine cycle is to convert thermal energy into electrical energy and this thermodynamic cycle is based on the rotation of a turbine

Waste Heat Recovery in Process Industries, First Edition. Hussam Jouhara.

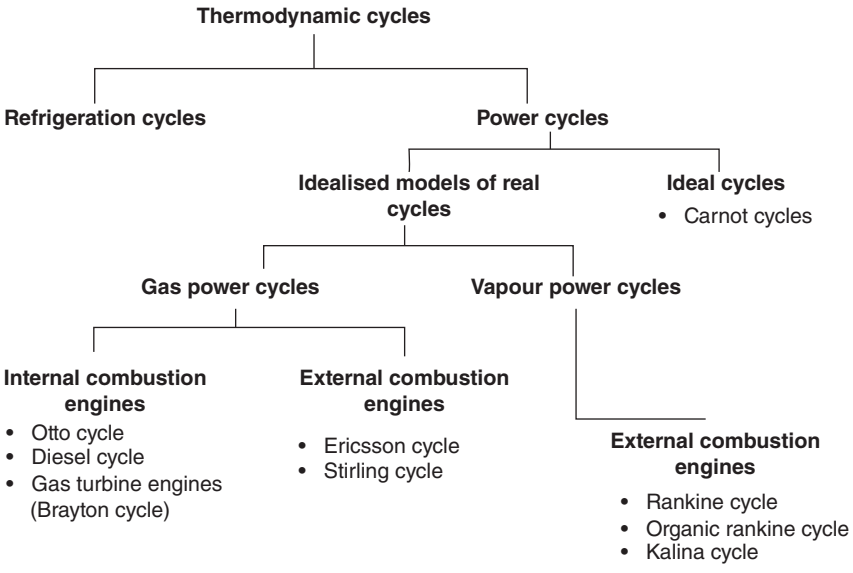

Figure 1.1 Map of all thermodynamic cycles.

fixed to a shaft and on to which an electrical generator is also located. In this way the mechanical energy of the turbine is converted into electrical energy, a more versatile and widely used form of energy. Rankine cycles and their different configurations are extensively used in thermal power plants such as nuclear, gas, oil, coal, geothermal, biomass, and concentrated solar power plants [1].

This section aims to present and explore in depth the Rankine thermodynamic cycle and following a general description of the cycle and a reminder of the Carnot cycle, different configurations will be presented and illustrated by means of diagrams and schematics. The driver for these various enhanced configurations always being to improve either the energetic or the exergetic efficiency of the cycle (or both). In this respect energy is a quantitative parameter and exergy a qualitative parameter, and we need to measure both of these in order to determine the total useful work we can extract from a thermodynamic system. The equations used to model such systems will be highlighted and explained as these formulas help us to understand the different parameters that influence the overall performance of a system. Real-life examples will also be used to clarify these explanations, and relevantly, a section of this document also explores the link between Rankine cycles and thermal power plants.

1.2.2 Thermodynamic Diagrams

In order to clearly understand the following sections of this document, it is important to be familiar with the basics of thermodynamics – the first and second laws as well as thermodynamic diagrams. Indeed, these diagrams are key aids in helping to develop a deeper understanding about how thermodynamic cycles function. The three main

physical parameters used to describe a thermodynamic system are the temperature (°C or K), the pressure (bar or Pa), and volume (m^3) and these give rise to three significant diagrams which can then be created to visualise the state of a fluid under specific conditions: the *P–V* diagram, the *T–V* diagram, and the *P–T* diagram. *P–V* diagrams plot pressure with respect to specific volume, *T–V* diagrams plot temperature with respect to specific volume, and *P–T* diagrams plot pressure with respect to temperature. Now as most thermodynamic cycles operate by making use of a phase change of the working fluid, such diagrams are also useful in that they graphically display values (of pressure, volume, and temperature) at which these phase changes occur, i.e. for a given material, the points when changes of state from say a solid to a liquid (the point of melting), or from a liquid to a gas (the point of vapourisation) occur – or their reverse processes – freezing and condensing. In fact, we can display the three parameters of pressure, volume, and temperature as a 'surface', Figure 1.2.

Firstly, you will note that we say 'surface' not 'solid', and that's because at any particular temperature and pressure the condition of a material would only lie on the surface and not above nor below it. For example, take a point for say water in Figure 1.2, diagram (i), on the vapour section of the diagram. We might try to imagine a point above this – i.e. one with an increased pressure – but water vapour cannot exist at this higher pressure at that temperature and volume. Nor will it exist at a lower pressure. It can only exist at the values of pressure, temperature, and volume that are shown on the given surface [2].

So, what are the three single-phase regions we can see on the diagrams? They are the gas/vapour region, the liquid region, and the solid region, and between these we have the transition or two-state phase change regions where the solids are melting or freezing, and the liquids are evaporating or condensing.

Now when considering a vapour and a gas, because the two terms are often confused – and to some extent are synonymous in that they both refer to a physical state that is not solid or liquid – we perhaps explain the need to differentiate them. Technically, below the critical temperature, a vapour and its liquid are in

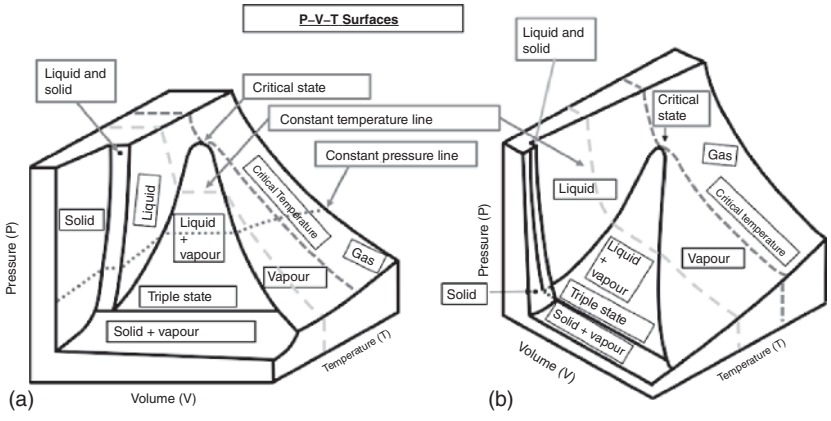

Figure 1.2 *P–V–T* diagrams. (a) A material heat contract on freezing. (b) A material that expands on freezing – water being the most well-known example.

'equilibrium' and a vapour can condense back to a liquid with a small change of pressure or temperature. Whereas a gas cannot condense to a liquid without changes in both pressure and temperature, and above the critical temperature line the liquid state does not exist at all! But what do we mean by being 'in equilibrium'?

Well, evaporation from the surface of a liquid or fluid takes place when the liquid molecules have enough momentum to overcome the cohesive forces within the fluid and escape into the space above it. To all intents and purposes, it becomes a gas, but because both the liquid and gas are present together it is more accurately known (in this state) as a vapour. If we now add heat to the liquid the momentum of the molecules increases, and more liquid evaporates. Similarly, a reduction in pressure above the liquid also reduces the momentum necessary for molecules to escape and so again evaporation is increased. But if the container which holds the liquid is sealed so that the evaporated vapour cannot escape, then the amount of liquid that can evaporate is finite. That is at any fixed value of temperature and pressure the amount of vapour will rise to a steady fixed amount and then no more can be added and the vapour is said to be 'fully saturated'. If any more molecules reach sufficient momentum to escape the surface then their number is exactly matched by those condensing back into the liquid, so an equilibrium or balance occurs between the two processes to limit the amount of vapour – or more correctly – the vapour pressure. Raise the temperature and the amount of vapour that can be maintained increases, and the 'fully saturated' line – the dome or bell-shaped line (in the earlier diagrams) illustrates the limit of this. So, to the right-hand side of the curve is where all the liquid will have evaporated and the liquid state cannot exist, whilst the left-hand side shows where all the solid has melted to liquid and the solid state can now longer exist. But under the curve is the region where both liquid and vapour exist together. Until that is, we reach the peak or 'critical point' or critical state where the distinction between the liquid and the gas no longer exists. Here the molecules are evaporating so rapidly that the density of the liquid and the vapour are equal and produce a 'supercritical fluid'; the point being that condensation of the gas will never occur above the critical point no matter how much pressure we apply.

But what else does the P–V–T diagram show us? For example, if we look at the liquid and solid regions, we will notice just how steep these surfaces are, and that's because, compared to gases, liquids and certainly solids are much harder to compress. So, at a particular temperature, if we increase the pressure it does not really change the volume or, conversely, the pressure will rise dramatically for a small change in volume. We can also note the transition phase between a solid and a vapour where 'sublimation' can occur. Dry ice is an example of such a material and is used where it is necessary to keep items cold but where any packaging will not get wet with liquid as the 'dry' ice warms up. We can also notice the triple state line where all three phases can coexist.

However, as useful as the P–V–T surface plot is to indicate the various states and transition phases of a substance they are a bit difficult to read-off from on to value scales. So, it is more usual to present thermodynamic information by means of two-axis diagrams that we briefly noted earlier. For example, the P–V diagram is the

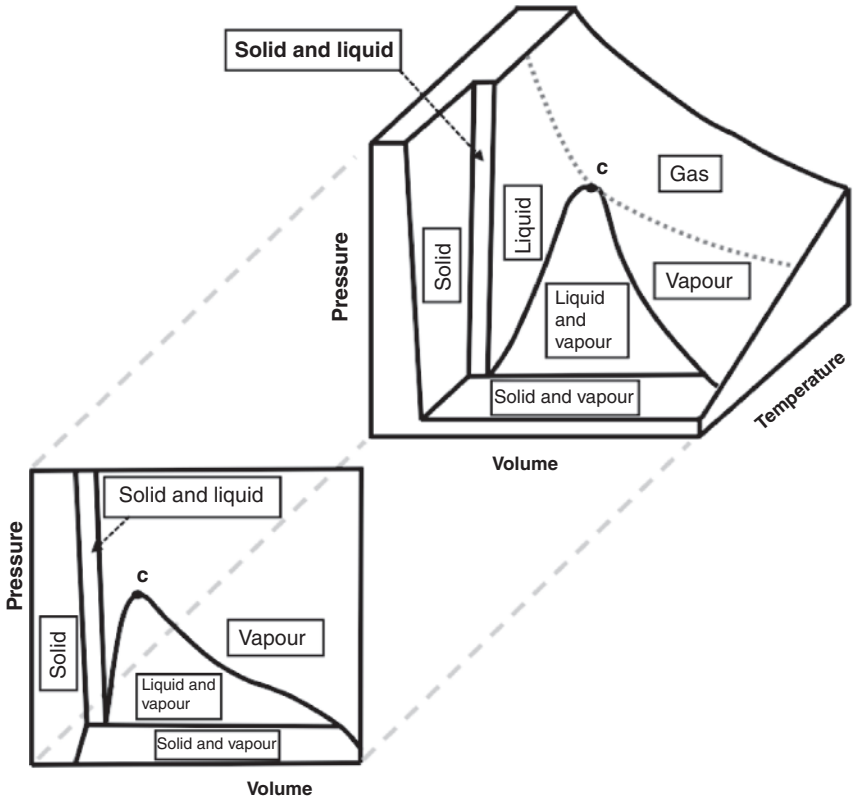

Figure 1.3 *P–V* perspective of a *P–V–T* diagram.

view we would obtain by looking at the surface from a pressure–volume perspective to see how a thermodynamic process changes with pressure and volume, Figure 1.3.

Usually we are only interested in the saturated liquid and saturated vapour areas, so our *P–V* diagrams are often 'truncated'. But in addition, our volume axis is more usually scaled in terms of *specific volume*, i.e. the cubic volume per kilogram of mass rather than just volume, because then, as an intensive property, the value does not depend on the size of the thermodynamic system. Hence, as we can see in Figure 1.4, the *P–V* diagram (also called a Clapeyron diagram) presents pressure as a function of the specific volume (m^3/kg), and on this diagram the left-hand side of the vapour dome shows the limit between the liquid region whilst the right-hand side shows the limit between the liquid/vapour region and the superheated vapour region. The diagram also denotes the plot of two isothermal lines or lines of constant temperature demonstrating that, inside the dome, the phase transition between liquid and vapour is a constant-pressure, constant-temperature process.

The other two diagrams that we can better visualise as two-dimensional graphs are the temperature–volume and the pressure–temperature diagrams as shown in Figure 1.5.

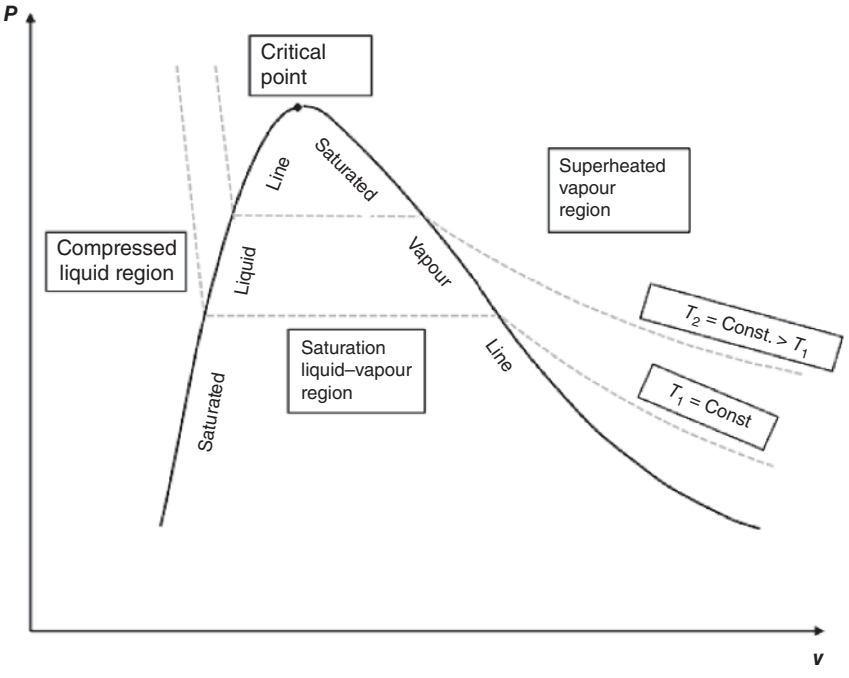

Figure 1.4 *P–V* diagram of a pure substance.

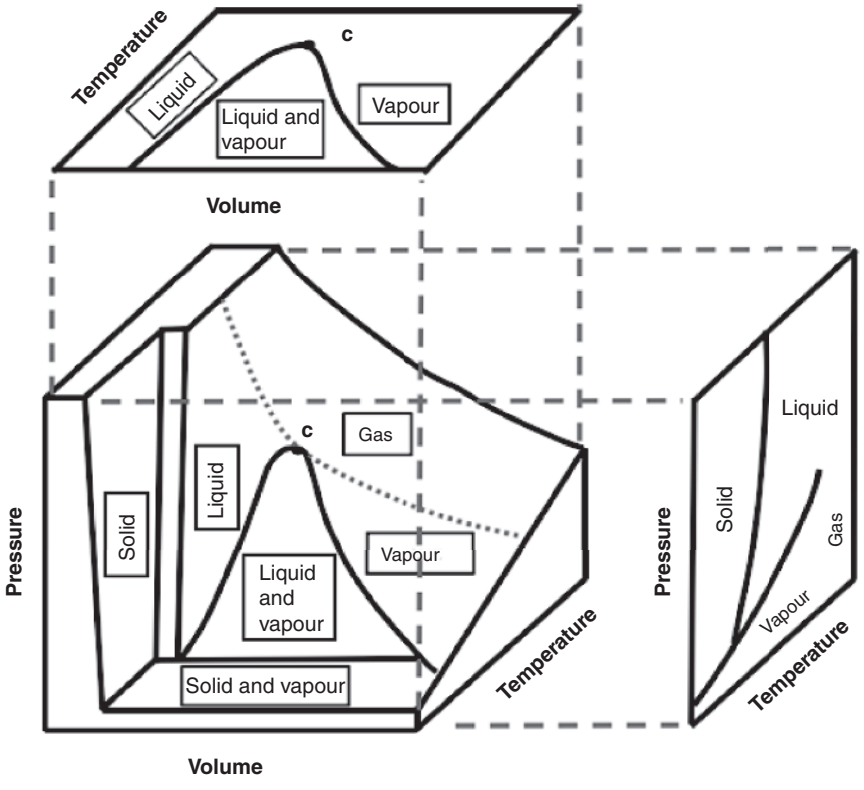

Figure 1.5 *T–V* and *P–T* perspectives of a *P–V–T* diagram.

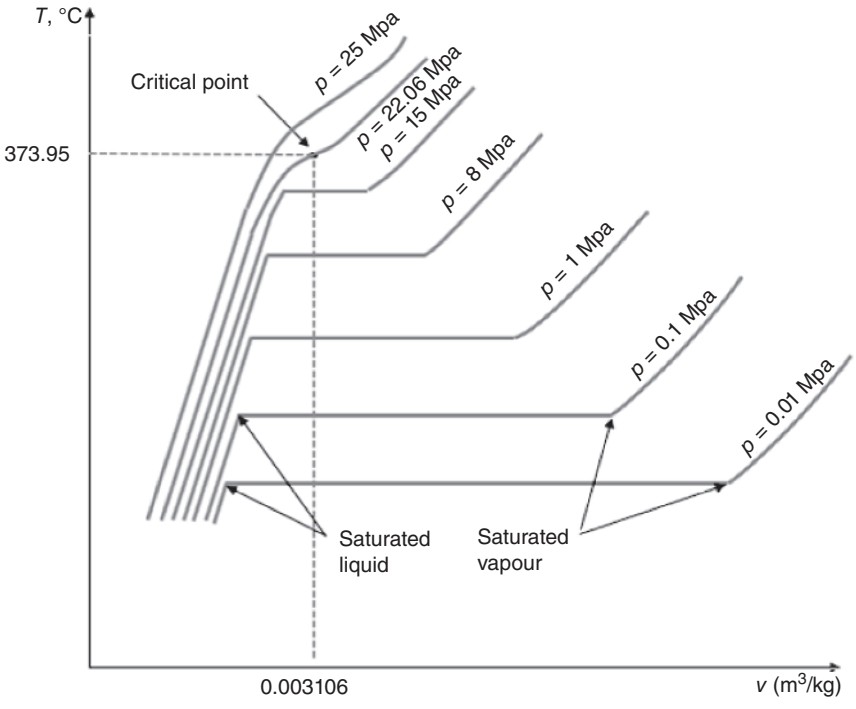

Figure 1.6 *T–V* diagram of a pure substance.

The vapour dome can also be seen on the *T–V* diagram in Figure 1.6, however, it is not directly visible on the *P–T* diagram in Figure 1.7 – which is also known as a phase diagram – in that for a given pressure and temperature the state of the substance is fully defined. As phase transitions occur under constant pressure and temperature for pure substances, alteration of the pressure or temperature will result in a phase change for the substance, the outcome being either a pure liquid or a pure vapour. For that reason, the liquid–vapour region is just a line on the *P–T* diagram and the vapour dome is not visible because, as we have already seen, a third dimension (the *P–V–T* diagram) is required to fully visualise the state of the fluid.

Two other thermodynamic variables are also very useful in describing a thermodynamic system from energetic and exergetic viewpoints, and these are the specific enthalpy h (kJ/kg) and the specific entropy s (kJ/kg K). Enthalpy (h) measures the total heat content of a system and is equal to the internal energy (i.e. the energy related to the molecular structure or state of the material and the degree of molecular activity) which is then added to the product of pressure and volume. In the analysis of systems that involve fluid flow, we often meet the combination of these two properties, defined from $h = u + PV$, where u represents the macroscopic energy of the non-flowing fluid and PV represents the energy needed to push and maintain the fluid flow around the system. But the second term, entropy, is defined as a measure of randomness of molecules, so what, we may ask, is its relevance to thermodynamics?

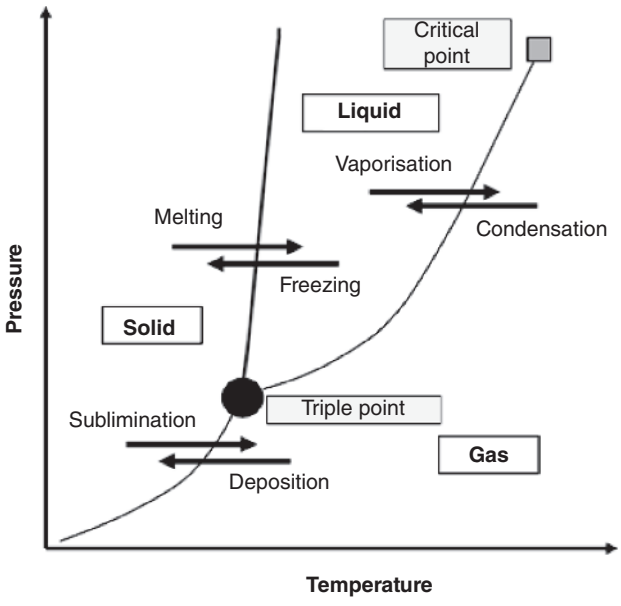

Figure 1.7 *P–T* diagram of a pure substance.

In fact, entropy is very relevant to thermodynamics and is the function of the quantity of heat that can be converted into work – and yes, it still does indicate the randomness of molecules. For example, suppose we put 100 J of energy into a system trying to convert this all into work can we then get 100 J back out? The answer of course is No! Some of that energy will be used in making more molecules move at random or increasing the momentum of those already in motion – that's why the entropy of a solid is less than that of a gas because gases have more molecules moving at random. Temperature increases the entropy of a material because as the temperature rises, the molecules spread out and take up more room – that is, they become more disordered. Pressure, on the other hand, has the opposite effect, it forces molecules closer together, so they become more ordered and entropy decreases. However, we should note that solids and liquids are nearly incompressible, so any entropy decrease is minimal.

So, in addition to those already mentioned, many other two- and three-dimensional diagrams can be plotted. For example, the *T–s* diagram (temperature as a function of specific entropy) and the *P–h* diagram (pressure as a function of specific enthalpy) are both very useful diagrams. An example of a temperature-specific entropy (*T–s*) diagram can be seen in Figure 1.8, and is often used to describe thermodynamic power cycles since the area drawn by the cycle on this form of diagram is equal to the work provided by it. Alternatively, a pressure–enthalpy (*P–h*) diagram, also called a Mollier diagram, might be used, as shown in Figure 1.9, to help describe receptor cycles such as refrigeration cycles.

These diagrams are also essential tools to aid understanding and for describing thermodynamic cycles, but in most cases when working with Rankine cycles the

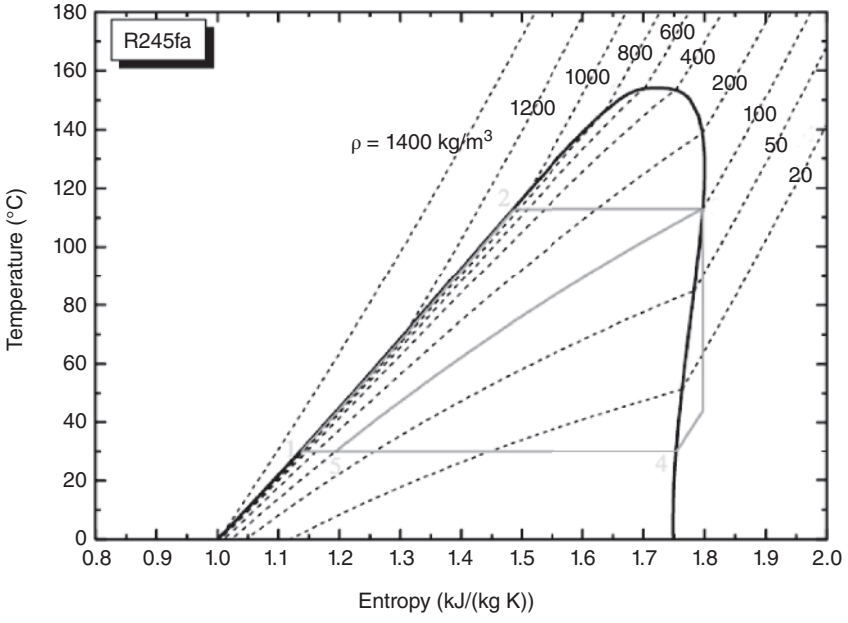

Figure 1.8 Example *T*–*s* diagram. Source: Based on Janie et al. [3].

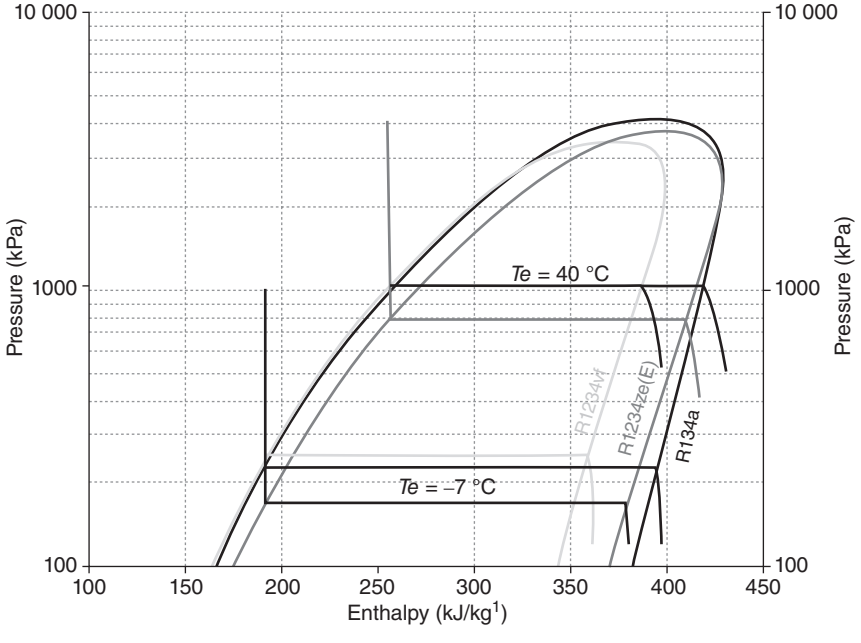

Figure 1.9 *P*–*h* diagram of refrigerants. Source: Sethi et al. [4].

T–s diagram is the most suitable. It will therefore be used extensively in the sections that follow.

1.2.3 The Carnot Cycle

Before we discuss the Rankine cycle and its application, we first need to consider its inspiration – the Carnot cycle [5].

Nicholas Léonard Sadi Carnot, the French mechanical engineer and physicist, is often described as the 'father of thermodynamics'. He published only one book, but in it he expressed the first successful theory of maximum heat engine efficiency and so laid the foundations, for what was then, an entirely new discipline. The Carnot cycle is therefore used as the common reference for every thermodynamic power cycle because even though the Carnot cycle is only a theoretical model, it does provide the standard as the most efficient engine possible. In other words, because the thermal efficiency of the Carnot cycle only depends on the absolute temperatures of the two heat reservoirs that drive the process, it gives us the upper limit of both energetic and exergetic thermodynamic cycle efficiency [6].

Most commonly, the working fluid used to explain the Carnot cycle is water and the cycle is divided into four phases as shown in Figure 1.10:

1. Isothermal expansion, (AB)
2. Isentropic (constant entropy) expansion, (BC)
3. Isothermal (constant temperature) compression, (CD)
4. Isentropic (constant entropy) compression, (DA)

Theoretically, these four processes are reversible, but in reality, reversible transformations do not exist because of, e.g. heat losses due to friction. The figure indicates a clockwise cycle and so is known as a Carnot 'power' cycle (power cycles are those which convert heat into mechanical work output whilst a 'heat pump' cycle transfers heat from lower to higher temperatures using mechanical work input).

Thermodynamic power cycles are the operating basis of heat engines, which currently supply much of the world's electric power and run almost all motor vehicles.

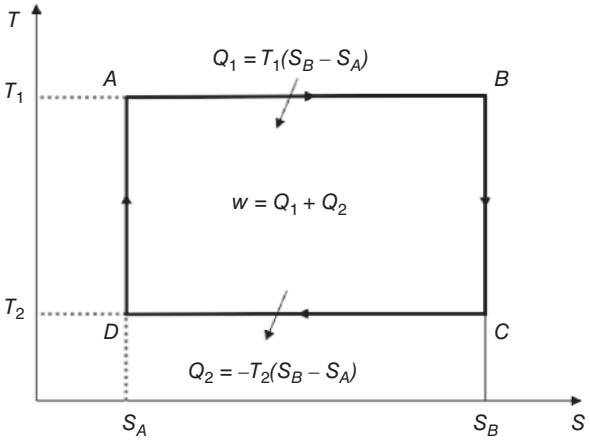

Figure 1.10 *T–s* diagram of the Carnot cycle.

Power cycles are classified according to the type of heat engine they model, e.g. we have the Otto cycle and the Diesel cycle for modelling internal combustion engines, the Brayton cycle for modelling gas turbines, and the Rankine cycle for modelling steam turbines.

Consider for a moment, the above *T*–*s* diagram as representing the Carnot cycle for an ideal or perfect gas turbine, i.e. one with no friction and the necessary heat transfers occurring without loss. What do the four stages of our cycle represent?

Essentially, we start with two 'heat reservoirs' with temperatures T_1 and T_2, respectively, and these have such a large thermal capacity that their temperatures are stable and unaffected by the cycle, which takes place as follows:

- Stage 1 (AB): Heat is transferred from the high-temperature reservoir (T_1) at constant temperature. During this phase, the entropy of the gas is increased by allowing it to expand and reduce its pressure and in doing so producing work on the surroundings – e.g. moving a piston or rotating a shaft within a turbine.
- Stage 2 (BC): During this stage of the cycle, it is assumed that the gas is thermally insulated from both the hot and cold reservoirs, so that they neither gain nor lose heat from the gas – i.e. the conditions are adiabatic (Greek ≡ without loss). Instead, the gas continues to expand (and do more work) further reducing the pressure and losing internal energy in an amount equal to the work done. Since this gas expansion occurs without any heat input, it cools to the 'cold' temperature T_2 but with the entropy unchanged.
- Stage 3 (CD): At this point the gas in now in thermal contact with the cold reservoir at temperature T_2, and work is then done on the gas to compress it – e.g. the piston is forced down or the gas passes into a compressor. In doing so, heat energy is transferred to the cold reservoir and the entropy of the system decreases by the same amount that it gained at Stage 1.
- Stage 4 (DA): It is assumed that the gas is thermally isolated from the hot and cold reservoirs (and any mechanical processes are frictionless) and further compression takes place, increasing the internal energy and so causing the temperature to rise back to T_1. This assumes that this temperature rise is solely due to the work added to the system and so the entropy remains unchanged. The gas is now back at the same state as the start of Stage 1.

As such, the work (kJ) provided by the thermodynamic cycle is given by:

$$W = \oint PdV = \oint TdS \tag{1.1}$$

In other words, the total work is given by integrating and thereby accumulating all the infinitesimally small changes in volume and pressure or entropy and temperature the gas makes on its journey around the cycle. Of course, the path taken by a real process differs somewhat from the ideal processes shown, but the idea here is to produce a perfect standard against which all other heat engines can be judged.

In a *T*–*s* diagram, the area under the upper portion of the figure represents the thermal energy absorbed during the cycle, whilst the area under the lower portion represents the thermal energy removed during the cycle – hence the area *inside*

the cycle will represent the difference between these two. However, since the internal energy of the system must return to its initial value, this difference must also represent the total amount of work performed by the system over one cycle. So, in definitive terms on the diagram, the absolute value of *all* this work ($|W|$) corresponds to the area of the rectangle. Or:

$$|W| = (T_1 - T_2) \cdot (S_B - S_A) \tag{1.2}$$

If Q_H represents the total amount of thermal energy transferred from the hot reservoir to the system (kJ), and Q_C represents the total amount of thermal energy transferred from the system to the cold reservoir (kJ), both as given by Eqs. (1.3)–(1.5):

$$Q_H = T_1 \cdot (S_B - S_A) \quad \text{and} \quad Q_C = T_2 \cdot (S_B - S_A) \tag{1.3}$$

Then the efficiency of the Carnot cycle can be defined as:

$$\eta = \frac{|W|}{Q_H} = \frac{Q_H - Q_C}{Q_H} = \frac{(T_1 - T_2) \cdot (S_B - S_A)}{T_1 \cdot (S_B - S_A)} \tag{1.4}$$

where, T_1 is the hot source temperature and T_2 is the cold source temperature (both are expressed in [K] Kelvin), and S_B and S_A correspond, respectively, to the entropy (kJ/K) at points B and A. From which, the overall efficiency will be given by the following equation:

$$\eta = \frac{T_1 - T_2}{T_1} = 1 - \frac{T_2}{T_1} \tag{1.5}$$

1.2.4 Ideal and Actual Rankine Cycles

The Carnot cycle is just a theoretical cycle. It is not possible to build a real engine working under such conditions because of real component *irreversibility*. For example, the transformations result in heat dissipation through friction. So, these transformations are defined as irreversible because once they have occurred, it is impossible to return them to their initial state. A reversible transformation is a succession of infinitesimal changes, each occurring *without* any energy loss, and in practice, this kind of transformation does not exist in the real world even though each component is designed in order to approach an irreversible behaviour.

The Rankine cycle is very similar to the Carnot cycle, the difference being that the reversible isothermal transformations are now replaced by isobaric (constant pressure) ones. In most cases, the working fluid is water too.

The ideal Rankine cycle is composed of two isobaric transformations and two adiabatic and reversible isentropic (constant entropy) transformations as shown in Figure 1.11. The four main components required for the Rankine cycle are a pump, a boiler, a turbine, and a condenser as shown in Figure 1.12.

The four transformations involved in the cycle are:

- 1–2: Isentropic compression (pump). The fluid (in liquid state) is compressed while the specific entropy remains constant.

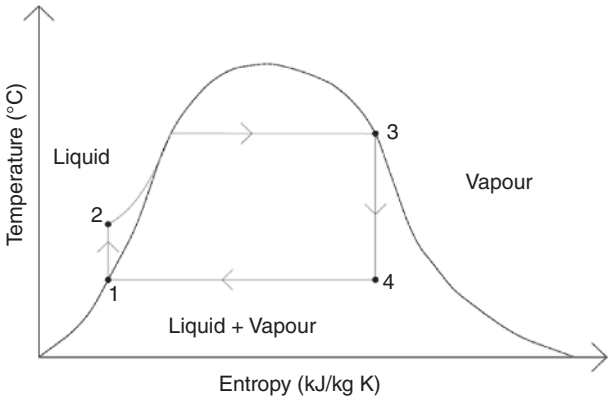

Figure 1.11 *T–s* diagram of the Rankine cycle.

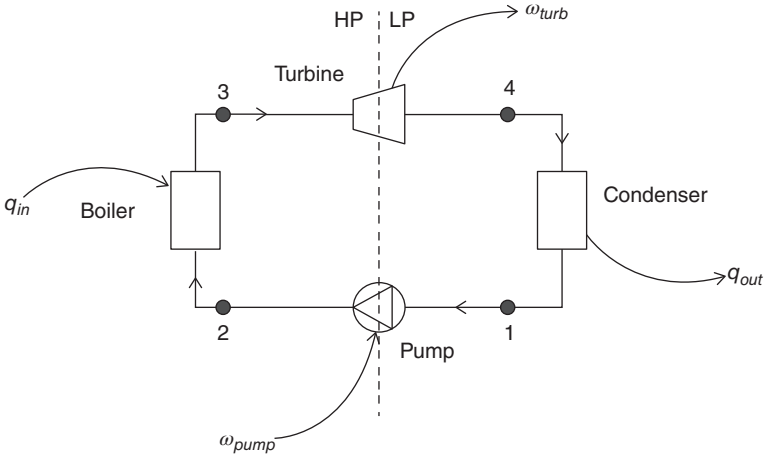

Figure 1.12 Schematic of the Rankine cycle.

- 2–3: Isobaric heat addition inducing vapourisation of the fluid (boiler), i.e. the fluid is heated under constant pressure and this results in a phase transition – the fluid changing from liquid to a mixture of liquid and vapour.
- 3–4: Isentropic expansion (turbine). The fluid is expanded through a turbine while the specific entropy again remains constant.
- 4–1: Isobaric heat rejection inducing liquefaction of the fluid (condenser), i.e. the fluid is cooled down under constant pressure and the vapour condenses.

1.2.4.1 Ideal Cycle

To describe the Rankine thermodynamic cycle, five physical variables are required:

1. The pressure P (Pa)
2. The temperature T (K)

3. The steam quality x, which represents the proportion of saturated vapour in a liquid/vapour mixture.

$$x = \frac{m_{vapour}}{m_{vapour} + m_{liquid}} \tag{1.6}$$

where, m_{vapour} and m_{liquid} correspond, respectively, to the masses (kg) of the vapour and liquid contained in the mixture. (For example, at point number 1 on the T-s diagram, $x(1) = 0$, i.e. the fluid is a fully saturated liquid.)

4. The specific enthalpy of the fluid h (kJ/kg)
5. The specific entropy of the fluid s (kJ/kg K)

Knowing the values of each of these variables at every point of the diagram is very useful, and helpfully the five variables are linked to each other through physical relationships.

Looking at the diagram it may not be obvious, but the cycle is divided in two pressure areas: high pressure (HP) and low pressure (LP) – these pressures being expressed in Pascal (Pa). Points 2 and 3 are in the HP section and points 4 and 1 are in the LP section, and as the transformation between 2 and 3 is isobaric: $P_2 = P_3$. (And similarly, for the same reason, $P_1 = P_4$.) Then the work provided to the system corresponds to the area of the quadrilateral shape drawn by the four points, but to calculate this work, the specific enthalpy of the fluid must be used. From which we can then determine the *specific work* (ω) – which corresponds to the amount of work delivered per unit of mass (kJ/kg).

The thermodynamic system is exchanging energy (work or heat) with its environment, and we should note here the convention that: heat transferred *to* a fluid is a positive quantity; heat transferred *from* a fluid is a negative quantity. It is necessary to note this because a Rankine cycle uses part of its work to compress the water, so will need to deduct the power put into the pump from the power output of the turbine in order to obtain the net work. Accordingly, the required work and heat parameters are determined from:

ω_{turb}, the work given by the fluid to the turbine (kJ/kg). It is negative as the fluid is giving work:

$$\omega_{turb} = h_4 - h_3 \tag{1.7}$$

ω_{pump}, the work given by the pump to the fluid (kJ/kg). It is positive as the pump gives work to the fluid:

$$\omega_{pump} = h_2 - h_1 \tag{1.8}$$

q_{in}, the heat given by the boiler to the fluid (kJ/kg). It is positive as the boiler gives heat to the fluid:

$$q_{in} = h_3 - h_2 \tag{1.9}$$

q_{out}, the heat given by the fluid to the condenser (kJ/kg). It is negative as the fluid rejects heat:

$$q_{out} = h_1 - h_4 \tag{1.10}$$

So, as the net work (ω_{net}) (kJ/kg) provided by the cycle is governed by:

$$\omega_{net} = \omega_{turb} + \omega_{pump} \tag{1.11}$$

Then the thermal efficiency (η_{th}) of the ideal Rankine cycle can be defined by:

$$\eta_{th} = \frac{|\omega_{turb}|}{q_{in}} \tag{1.12}$$

And hence the overall efficiency (η) of the ideal Rankine cycle can be defined by:

$$\eta = \frac{|\omega_{net}|}{q_{in}} = \frac{|\omega_{turb}| - \omega_{pump}}{q_{in}} \tag{1.13}$$

Substituting Eqs. (1.4)–(1.6) then leads to:

$$\eta = \frac{|h_4 - h_3| - (h_2 - h_1)}{h_3 - h_2} = \frac{h_3 - h_4 - (h_2 - h_1)}{h_3 - h_2} \tag{1.14}$$

In practice however, compared to the output of the turbine, the work input to the pump is very small. In which case, if ω_{pump} can be neglected compared to the other coefficients, we arrive at the useful approximation of:

$$\eta \approx \frac{h_3 - h_4}{h_3 - h_2} \tag{1.15}$$

So to estimate the efficiency of the system, we can also use the first law of thermodynamics which states that the net energy of a system is equal to 0, i.e.

$$\omega_{turb} + \omega_{pump} + q_{in} + q_{out} = 0 \tag{1.16}$$

And further assuming ω_{pump} is neglectable compared to the other coefficients gives:

$$|\omega_{turb}| \approx q_{in} - |q_{out}| \tag{1.17}$$

From which the efficiency of the ideal Rankine cycle can now be estimated from the following formula:

$$\eta \approx \frac{|\omega_{turb}|}{q_{in}} \approx \frac{q_{in} - |q_{out}|}{q_{in}} = 1 - \frac{|q_{out}|}{q_{in}} \tag{1.18}$$

Practically the efficiency of the ideal Rankine cycle is necessarily lower than the efficiency of the theoretical Carnot cycle even using the same hot and cold sources. In addition, the cycle presented in this section is still an ideal cycle, and the actual cycle used, for instance, for power plant analysis is slightly different.

1.2.4.2 Superheated Rankine Cycle

In the conventional Rankine cycle, the isentropic expansion occurs in the wet steam domain (transformation 3–4 in Figure 1.11). To explain, when a boiler heats water, bubbles breaking through the water surface pull tiny droplets of water into the steam which then becomes partially wet ('wet steam') from the added liquid. As water is the working fluid, it can cause damage to the turbine due to corrosion. Therefore, to mitigate this in power plants, the vapour is superheated to remove any moisture that it contains. Steam dryness is important because it has a direct effect on the total

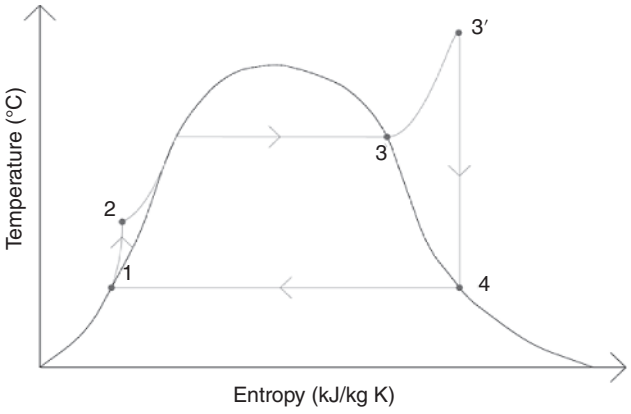

Figure 1.13 *T–s* diagram of the superheated Rankine cycle.

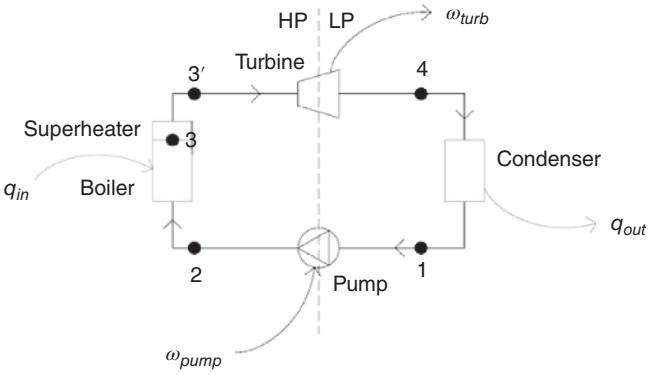

Figure 1.14 Schematic of the superheated Rankine cycle.

amount of transferable energy contained within the steam. For example, saturated steam (100% dry) contains 100% of the latent heat available at that pressure.

The result of this can be seen in the shape variation for the *T–s* diagram of the cycle as shown in Figure 1.13. In this case, the cycle is still a Rankine cycle and is sometimes called Hirn (or Rankine with superheating) cycle, so one extra component is required: the superheater as shown in Figure 1.14. However, in most cases, the boiler and the superheater are the same component.

Overheating is also interesting because it increases the amount of work given to the turbine. As we can see on the *T–s* diagram, the area of the superheated cycle is bigger than the area of the classical Rankine cycle. And in this way, for a same power output, the water flow rate can be lower for the Rankine–Hirn cycle than for a classical Rankine cycle, so improving the energetic efficiency of the system. Unfortunately, superheating also increases the irreversibility of the cycle and therefore, correspondingly, the exergetic efficiency of the system is regrettably reduced.

The main difference between the two cycles is that the heat given to the fluid by the boiler/superheater enhances the superheated cycle. On the *T–s* diagram, this

extra heat addition corresponds to the transformation 3–3′. This way, the expansion of the fluid then occurs within a superheated steam domain and corresponds to the transformation 3′–4 on the diagram. Furthermore, this transformation is assumed to display a greater degree of isentropic change and so is shown as a vertical line on the diagram, contrary to the transformation we now see between 1 and 2.

The efficiency of the superheated cycle is given by the same equation as the classical Rankine cycle (Eqs. (1.13) and (1.14)) – the difference being in the position of point 3′ (instead of 3), i.e.

$$\eta = \frac{h'_3 - h_4 - (h_2 - h_1)}{h'_3 - h_2} \tag{1.19}$$

1.2.4.3 Actual Rankine Cycle

The *actual* Rankine cycle is the best cycle with which to model the transformations occurring within a power plant as it is the one which takes both system irreversibility and system imperfections into consideration.

In this cycle, friction caused by the moving fluid induces pressure losses or heat loss, and as a result the isobaric transformations described in the ideal Rankine cycle are not exactly isobaric in the actual cycle. Pressure drops in the condenser and in the turbine reduce the area of the cycle, as shown on the *T*–*s* diagram in Figure 1.15. Hence, the specific work of the cycle is lower for the actual cycle than for the ideal cycle. Furthermore, the isentropic transformations described in the ideal cycle are not reversible, as they are in the actual cycle: irreversibility deteriorates the performances of the pump and of the turbine. Hence, the exergetic efficiency is reduced.

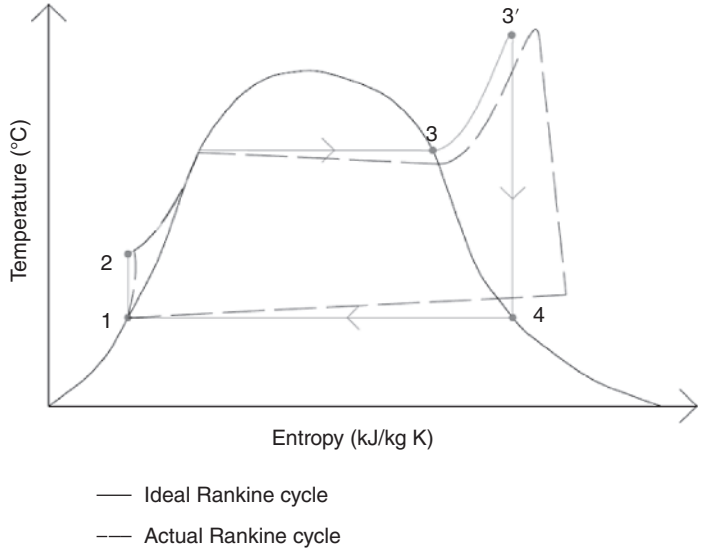

Figure 1.15 Ideal Rankine cycle vs. actual Rankine cycle on a *T*–*s* diagram.

In thermodynamics, *reversibility* defines the best theoretical work process, i.e. as the name suggests, one which can proceed in both the forward and the reverse directions – but with the key point that the system and its parameters are returned to their initial states at the end of the reverse process. *Irreversibility* is a concept that recognises that processes are not perfect, losses occur, and in thermodynamics these are quantified by:

- The difference between the work output (or input) of a reversible process and the actual work process
- The entropy a system generates during a process.

Fortunately, the efficiency of the cycle can be given by the same expression as the ideal Rankine cycle (Eq. (1.14)). However, the values of the specific enthalpy are not the same as those in the ideal Rankine cycle.

To make comparisons between the compression and expansion transformations of an actual cycle to the isentropic transformations of the ideal cycle, an isentropic efficiency needs to be introduced and this comes within the term the *adiabatic efficiency,* and a series exists to define isentropic efficiencies for turbines, compressors, and nozzles. For instance, the isentropic efficiency of the expansion transformation in the turbine is defined as follows:

$$\eta_{i,turb} = \frac{\text{Energy given to the turbine with the actual transformation}}{\text{Energy given to the turbine with the isentropic transformation}} \tag{1.20}$$

As an example, Figure 1.16 compares the actual and the isentropic expansion of the vapour in a turbine on a *h*–*s* diagram, and to accommodate the difference, an adaption is made to Eq. (1.20) in order to express this adiabatic efficiency using specific enthalpy as follows: If we start by assuming that vapour is an ideal gas, then it is possible to calculate the pressure, temperature, enthalpy, and entropy of the fluid using the Laplace's equation:

$$P^{1-\gamma} \cdot T^{\gamma} = \text{Constant} \tag{1.21}$$

In this equation, γ is the heat capacity ratio, a dimensionless coefficient.

Knowing the temperature and pressure values at the inlet and the pressure at the outlet of the turbine, it is then possible to calculate the temperature value that would be reached if the transformation was truly isentropic. Then once T_{2s} is calculated, and h_1, h_{2a}, and h_{2s} deduced from thermodynamic tables, the adiabatic efficiency of the turbine can be calculated. The isentropic efficiency of the pump is often also used to take the irreversibilities of the pump into consideration.

It is given by the following equation:

$$\eta_{i,pump} = \frac{\text{Isentropic pump work}}{\text{Actual pump work}} \tag{1.22}$$

And the process starts by assuming the water is incompressible, which then leads to:

$$\text{Isentropic pump work} = \Delta h = V \cdot \Delta P \tag{1.23}$$

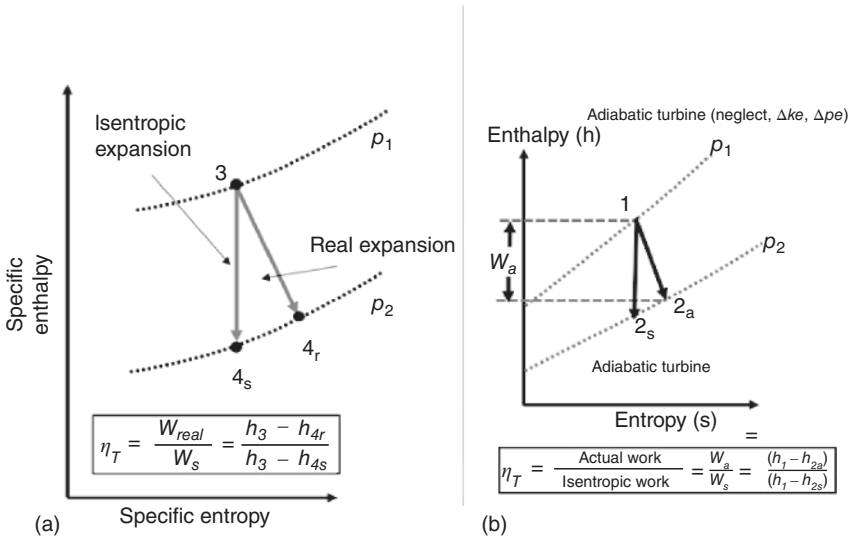

Figure 1.16 Adiabatic efficiency of a turbine.

In this equation, V is the specific volume of water (m^3/kg). It is constant along the transformation if the fluid is supposed incompressible. The pressure difference, ΔP, is expressed in Pascal (Pa). Again, knowing the actual inlet and outlet temperatures/pressures of the pump, it is possible to calculate the actual pump work, and this corresponds to the variation of enthalpy. All from which the isentropic efficiency of the pump can be deduced.

So, when using equations for the ideal cycle, it is important to be aware of the real efficiencies for all the components. For example, the turbine and the pump both also have a mechanical efficiency. All these imperfections will be described in depth in the power plant section so that we can better express the real link between the heat input and the electricity output produced by a plant.

1.2.4.4 Improvements to the Rankine Cycle

The Hirn cycle has a greater efficiency than the Rankine cycle and this is expected since the expression for Carnot's efficiency (Eq. (1.5)) illustrates that the higher the hot source temperature, the greater the efficiency. It is also true for the Rankine cycle (Eq. (1.18)).

Therefore, increasing the temperature of the hot source is a way of improving the efficiency of the Rankine cycle, but it also results in an increase in the boiler pressure. In the past, the boiler pressures were limited because of the materials used [7]. Over time however, the upper limit on boiler pressure rose and currently, with advances in metallurgy, it is possible to go over the critical pressure of water (220.6 bar) and some coal-fired power plants today are operating with boiler pressures around 300 bar.

Moreover, other improvements can also be made to improve the efficiency of the cycle, and these main improvements are presented within this section.

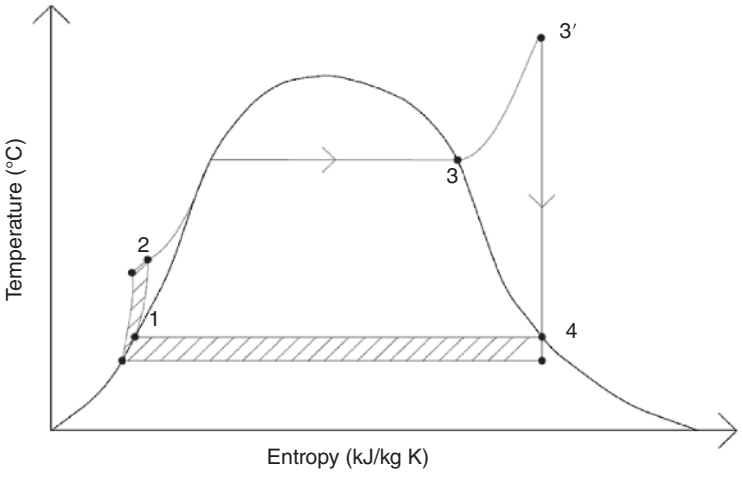

Figure 1.17 Effects of decreasing the LP on the Rankine cycle.

Decreasing the LP As we have noted, on our diagrams the lines drawn between the different points of the cycle represent thermodynamic processes and furthermore, the area enclosed by these lines corresponds to work provided by the system. This means that trying to increase the amount of work given by the system is the graphical equivalent to expanding this area, and one way to achieve this is to decrease the pressure of the system. As we can see, the lower the pressure, the lower the bottom line (condensation phase) of the cycle, i.e. the area of the cycle is increased (Figure 1.17).

In addition, if the pressure decreases, it leads to an increase in net work compared to the increase in heat input ($\Delta\omega_{net} > \Delta q_{in}$), then the efficiency of the system will also increase. However, as we see in Figure 1.17, decreasing the pressure of the system can result in introducing lower quality steam into the turbine, i.e. we run the risk or moving back into the wet steam domain – the further the point is from the saturated vapour curve, the lower the steam quality. Low steam quality can result in turbine deterioration due to corrosion and a subsequent decrease in mechanical efficiency. Hence, the pressure of the Rankine cycle must be set as low as possible in order to improve the energetic efficiency of the system – but not too low to still ensure a high steam quality.

Increasing the HP We might therefore conclude that increasing the pressure will also have a beneficial effect, but increasing the pressure actually keeps the work of the cycle roughly steady. Figure 1.18 shows the effect of this increase on a *T*–*s* diagram. Helpfully, the area of the cycle increases on the top part of the cycle (area shaded on the diagram) but unfortunately, it then also decreases on the right part of it (area shaded on the diagram) so the net gain is very small. Nonetheless, as the average temperature of the hot source increases, so increasing the pressure of the cycle has a positive effect on the cycle's efficiency. However, this increase then leads to a lower steam quality at the end of the expansion phase (point 4) which, as we have seen, can affect turbine operation.

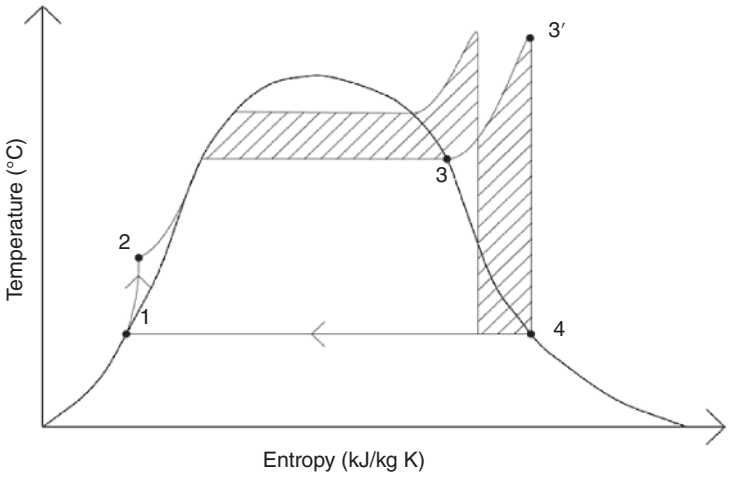

Figure 1.18 Effects of increasing the HP on the Rankine cycle.

To sum up, both the HP and the LP values must be carefully chosen so as to ensure that we achieve the highest possible energetic efficiency whilst still ensuring that we maintain high steam quality at the end of the expansion phase. Of course, it does not help that with modern plants, the LP and HP can vary as functions of time. But by using controllers which adjust these values (LP; HP) by taking into account external condition – such as outside temperature and pressure – we can ensure optimal performance.

Rankine Cycles with Reheat As we have seen, steam quality is a very important factor in the Rankine cycle. So, in order to avoid low steam quality at the end of the expansion phase, reheat cycles were introduced in the first part of the twentieth century. This category of cycle also involves having two turbines positioned on the same shaft as shown in Figure 1.19. The first turbine allows the expansion of the steam coming from the superheater from HP to a medium pressure (MP) (Figure 1.20), and this steam is then reheated and expanded in the second turbine from MP to LP. The main advantage of the reheat is to increase the steam quality to ensure a steadier thermodynamic efficiency.

Rankine cycles with reheat also ensure a higher overall mechanical efficiency by using two turbines for the cycle compared to only using one. In this configuration, the overall efficiency of the cycle is given by:

$$\eta = \frac{|\omega_{turb1}| + |\omega_{turb2}| - \omega_{pump}}{q_{inB} + q_{inR}} = \frac{|h_4 - h'_3| + |h_6 - h_5| - (h_2 - h_1)}{h'_3 - h_2 + h_5 - h_4}$$
$$= \frac{h'_3 - h_4 + h_5 - h_6 - (h_2 - h_1)}{h'_3 - h_2 + h_5 - h_4} \tag{1.24}$$

where, q_{inB} corresponds to the heat (kJ/kg) provided by the boiler to the fluid and q_{inR} corresponds to the heat (kJ/kg) provided by the reheater to the fluid (In real-life power plant, the boiler and the superheater use the same heat source.)

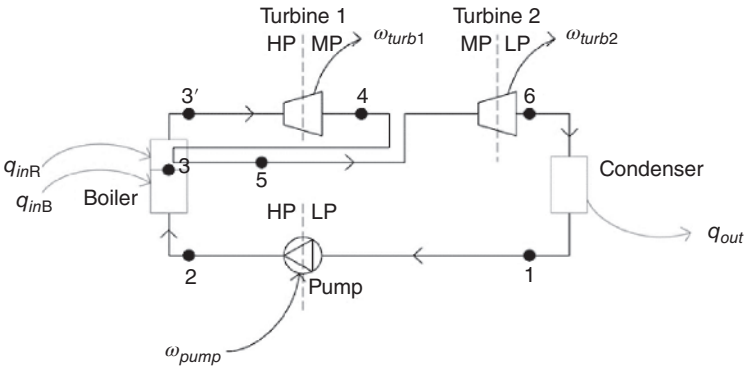

Figure 1.19 Schematic of the Rankine cycle with reheat.

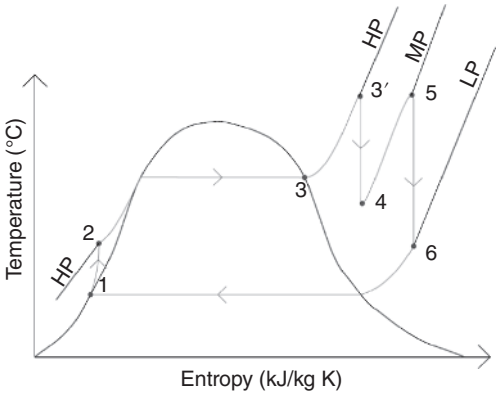

Figure 1.20 *T–s* diagram of a Rankine cycle with reheat.

1.2.4.5 Regenerative Rankine Cycles

To improve energetic and exergetic efficiency of the thermodynamic cycle, the regenerative Rankine cycles extracts a portion of the steam from the turbine to heat the fluid before it is sent to the boiler. This results in a small reduction in the work provided to the turbine but a substantial reduction in the heat input, because the heating phase creates entropy and thus irreversibility if this is all provided by the boiler. The portion of steam used therefore helps the boiler heat the fluid, reducing the fuel required by the boiler and hence both energetic and exergetic efficiencies improve. Furthermore, the average temperature of the heat input by the boiler is increased and this also results in a higher energetic efficiency [8].

Regenerative cycles require a new component. A feed water heater (FWH) also called a *regenerator* is required, its role being to heat the feed water before it enters the boiler. There are two different kinds of regenerative cycle: the open FWH cycle and the closed FWH cycle.

Open FWH cycles use an Open FWH. As seen in Figure 1.21, this component mixes the liquid delivered from pump 1 with the extracted steam arriving from turbine. It corresponds to point 6 on the *T–s* diagram shown in Figure 1.22.

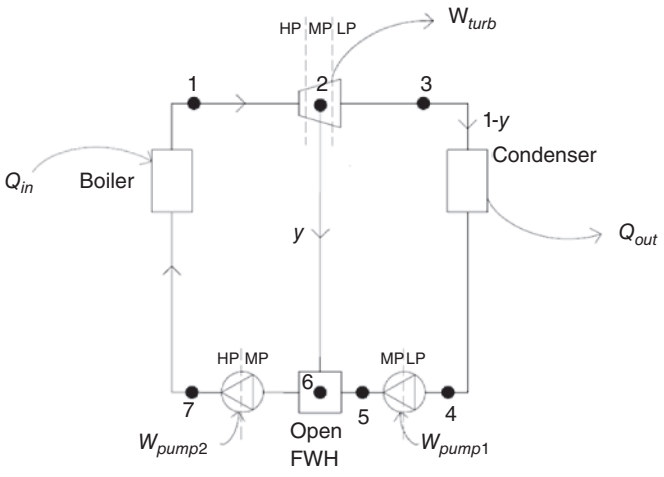

Figure 1.21 Schematic of a Rankine cycle with reheat and one open FWH.

Figure 1.22 *T–s* diagram of a Rankine cycle with reheat and one open FWH.

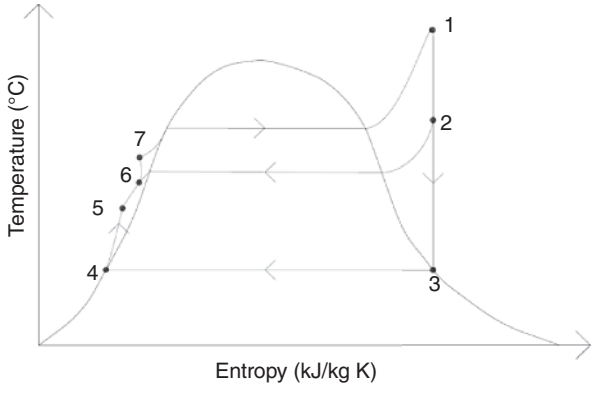

As the mixing takes place at MP, pump 1 is only required to compress the fluid from LP to MP. Hence, after this mixing phase, a second pump is then required to increase the pressure to HP. This second compression phase corresponds to the transformation 6–7 on the *T–s* diagram (Figure 1.21).

Now if y represents the mass proportion of steam extracted from the compressor, and:

$$y = \frac{\dot{m}(2 \rightarrow 6)}{\dot{m}(1 \rightarrow 2)} \tag{1.25}$$

where $\dot{m}\,(2 \rightarrow 6)$ corresponds to the mass flow rate (kg/s) between points 2 and 6, and $\dot{m}(1 \rightarrow 2)$ corresponds to the mass flow rate between points 1 and 2.

Then the overall efficiency of the open FWH cycle is given by:

$$\eta = \frac{|\omega_{turb}| - \omega_{pumps}}{q_{inB}} = \frac{(h_1 - h_2) + (1-y)(h_2 - h_3) - (1-y)(h_5 - h_4) - (h_7 - h_6)}{h_1 - h_7} \tag{1.26}$$

This efficiency is always greater than the efficiency of the ideal Rankine cycle given in Eq. (1.14). Indeed, the greater the number of regenerators, the higher the cycle efficiency.

So, writing the energy balance of the open FWH leads to:

$$y \cdot h_2 + (1 - y) \cdot h_5 = h_6 \tag{1.27}$$

Now the open FWH requires two pumps: one at its inlet and one at its outlet, but to avoid this multiplication of pumps in a power plant, it is possible to use a closed FWH. Moreover, closed FWHs are more reversible than open ones.

A closed FWH has the same role as the open, but there is no mixing of the extracted steam with the feed water. This way the extracted steam and the feed water can have different pressures, the FWH then operating as a shell and tube heat exchanger. It is more expensive and complex than an open FWH, but requires less area and maintenance is reduced because of the lower number of pumps.

In the closed FWH system the extracted steam is cooled and turned into condensate and two options are available to reinject this condensate in to the cycle as shown Figures 1.23 and 1.24.

The 'drain cascaded backward' technology is the cheapest way to reinject the condensate, and with this configuration a steam trap is first used to reduce the pressure from MP to LP, which then reintroduces the condensate to the condenser as shown in Figures 1.25 and 1.26. However, the overall adiabatic efficiency of a steam trap is lower than the average efficiency of a pump, so the *drain pump forward* technology offers better performance. In fact, in the steam trap, because the pressure drops suddenly, exergy is destroyed and so is not reversible. On the other hand, in the pump (of the pump forward technology), the pressure of the fluid is increased more slowly resulting in a process more closely resembling a reversible process and resulting in less exergy reduction.

Reiterating, the drain pumped forward technology is more expensive and requires more maintenance. In the configuration, a pump is used to increase the condensate

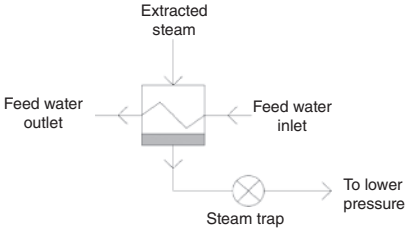

Figure 1.23 Schematic of the drain cascaded backward technology.

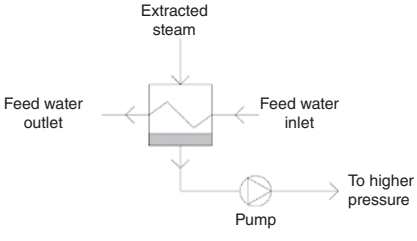

Figure 1.24 Schematic of the drain pump forward technology.

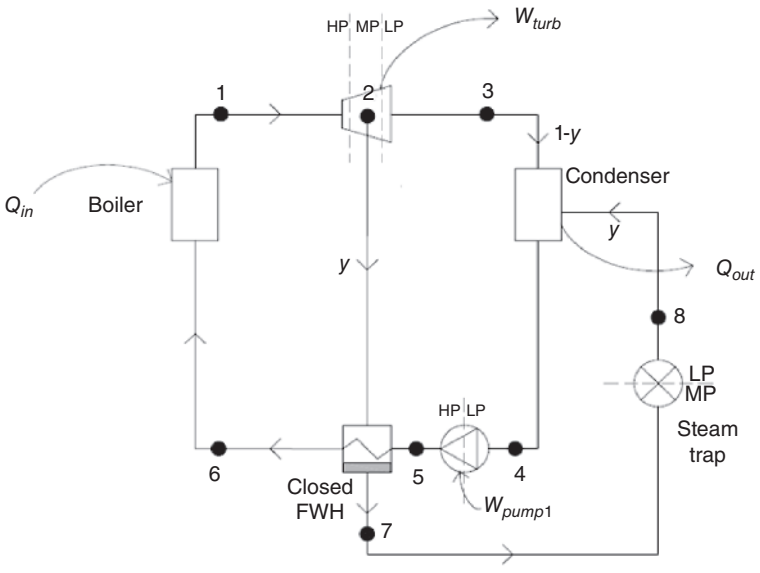

Figure 1.25 Schematic of a Rankine cycle using closed FWH and drain cascaded backward technology.

Figure 1.26 *T–s* diagram of a Rankine cycle using closed FWH and drain cascaded backward technology.

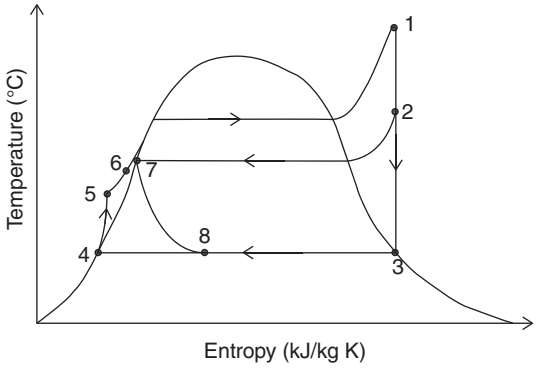

pressure from MP to HP, and then the condensate is mixed with the feed water in a mixing chamber, as shown in Figure 1.27. However, this process does produce higher energetic and exergetic efficiencies because the pump creates less irreversibility than a steam trap.

In a closed FWH (using the same notations as Figure 1.27), the energy balance leads to:

$$y \cdot (h_2 - h_7) = (1 - y) \cdot (h_6 - h_5) \tag{1.28}$$

This expression for the efficiency of the closed FWH cycle is the same as the expression for the efficiency of an open FWH. However (in Figure 1.27 for example), the benefit of the closed FWH is that the specific energy given by the boiler (q_{in}) is equal

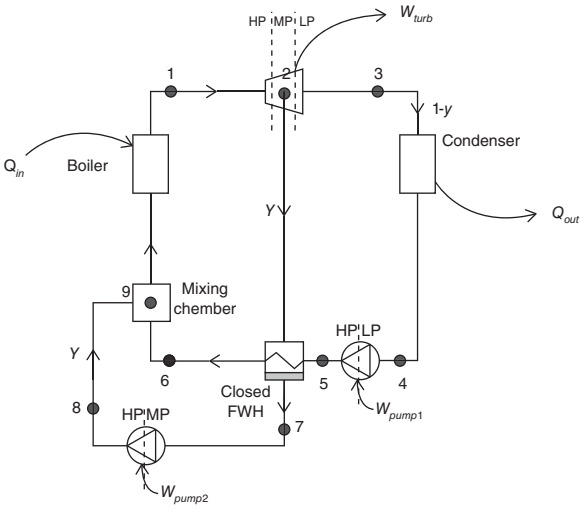

Figure 1.27 Schematic of a Rankine cycle using closed FWH and drain pumped forward technology.

to $h_1 - h_9$. Without it, the specific energy would have been $h_1 - h_5$, and since $h_5 < h_9$, q_{in} is reduced with a closed FWH.

Regenerative Rankine cycles are widely used in electrical power plants – the number of FWH systems varying from 6 to 10 and, in most of the cases, both open and closed FWH configurations can be used in the same plant.

1.2.4.6 Cogeneration

Cogeneration is the generation of two types of energy using only one source of primary energy. In most cases, cogeneration processes produce both electrical and thermal energies and so cogeneration is also known as *combined heat and power* (CHP).

The aim of a Rankine cycle-based power plant is to create electrical energy through the rotation of a steam turbine. However, in the process we also waste a lot of heat. Cogeneration offers a solution to utilise the thermal energy of this waste heat, thereby increasing the overall efficiency of the whole process. In Europe in 2011, 11% of heat and electricity requirements were produced with cogeneration plants [9].

Here is an example to better understand the benefits of cogeneration. To produce 350 kW electrical (kW_e) and 530 kW thermal (kW_{th}), a cogeneration power plant with an electrical efficiency (Eq. (1.29)) of 35% and a thermal efficiency (Eq. (1.30)) of 53% would use 1000 kW of primary energy. By comparison, a high efficiency power plant, such as a combined cycle gas turbine (CCGT) power plant, with an efficiency of 55% combined with a high efficiency boiler at an efficiency of 90% would require 1225 kW of primary energy [10]. Hence, in this example, the CHP cogeneration power plant saves 18% of the primary energy in comparison to the separate production of heat and electricity. The benefits of cogeneration are therefore: energetic, economic, and environmental.

$$\eta_e = \frac{P_{elec}}{P_{in}} \tag{1.29}$$

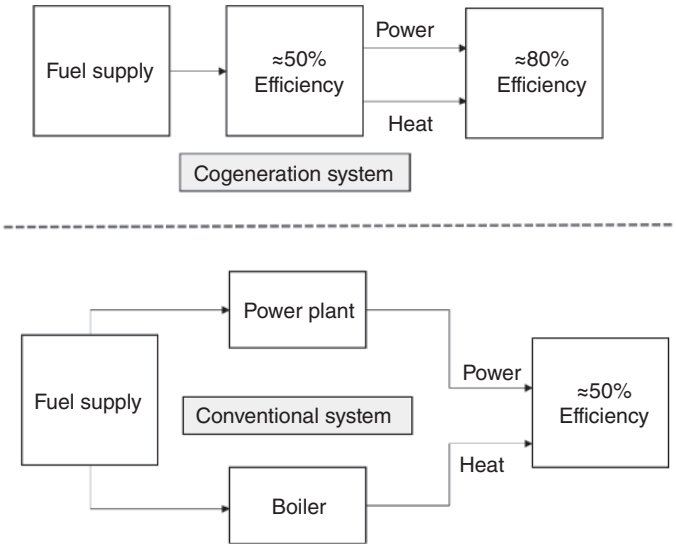

Figure 1.28 Cogeneration vs. conventional system.

$$\eta_{th} = \frac{P_{thermal}}{P_{in}} \tag{1.30}$$

where, P_{elec} is the electrical power output, $P_{thermal}$ is the thermal power output, and P_{in} is the total power input (kW). In this example, the overall efficiency of the cogeneration plant is 88% whereas the overall efficiency of the conventional system is 72%. Furthermore, the overall system efficiency is further reduced during the delivery of this conventional electrical power owing to approximately 10% (or more) power loss in transmission.

In its general application therefore, Figure 1.28 illustrates why cogeneration is a better solution than conventional systems for producing both heat and electricity. Notwithstanding other advantages, the average overall efficiency of a cogeneration plant is higher than the average overall efficiency of a conventional system.

The efficiency of a cogeneration power plant is given by:

$$\eta_{cogen} = \frac{P_{elec} + P_{thermal}}{P_{in}} \tag{1.31}$$

Although cogeneration power plants can use fossil fuel or uranium as their combustible, it is also possible to use renewable forms of energy such as solar, biomass, or geothermal.

The main disadvantages of a cogeneration power plant are that: (i) the production of electrical energy involves the production of a large quantity of thermal energy – which is sometimes difficult to use – and (ii) electrical energy is much more versatile in comparison with thermal energy. Common ways to harness the thermal energy produced by cogeneration plant is to use it for industrial applications or for district heating, e.g. through a heat network [11], but other applications are also practical such as using the heat to warm the water of a swimming pool. It is

also possible to use a portion of the thermal heat output to produce cooling energy through a *sorption* chiller, this process being called trigeneration [12].

A cogeneration Rankine cycle requires a heat exchanger to recover heat from the fluid and in one of several possible cogeneration configurations, heat is recovered directly from the condenser – in which case, the cogeneration plant is operating as a back pressure plant. The temperature of the heating stream is directly linked to the pressure of the fluid within the condenser, this pressure being controlled by a valve. The higher the pressure of the condenser, the higher the temperature of the heating stream. However, we must be careful because the higher the pressure within the condenser, the lower the efficiency of the thermodynamic cycle.

So, to avoid influencing the LP of the cycle, it is also possible to extract a fraction (y) of the steam coming from the turbine to add heat to the heating stream. In this case, the heat recovery does not influence the LP of the system. Unfortunately, as the mass flow rate in the turbine is reduced, the work delivered by the fluid to the turbine is also reduced. As the fraction extracted is controlled with a valve, different heating needs can be met by varying this. Figure 1.29 is a schematic of this kind of cycle. Point 6 in the figure is the mixing chamber.

Figure 1.30 represents the T–s diagram of this cogeneration cycle, which is very similar to the T–s diagram for the regenerative Rankine cycle with an open FWH. The difference between those two cycles being that, with the open FWH configuration, the latent heat from the extracted steam is entirely given to the feed water for the regenerative cycle, whereas with the cogeneration cycle, a fraction of this latent heat is given to the heating stream. The value of this fraction is a function of the temperatures and flows within the heat exchanger – which can vary with the time. Hence, the position of point 2′ on the T–s diagram is variable. For example, if the process heater recovers 100% of the latent heat from the extracted steam, then this point will be on the left side of the vapour dome. However, if it is less than 100%, the point will be under the vapour dome, in which case, the rest of the latent heat is given to the feed water and the mixing chamber acts as an open FWH.

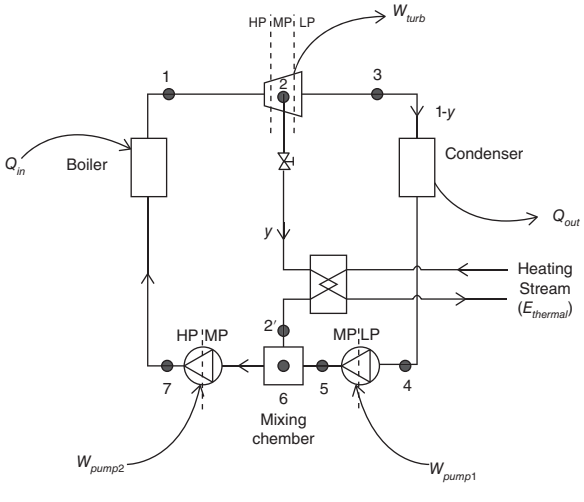

Figure 1.29 Schematic of a cogeneration Rankine cycle.

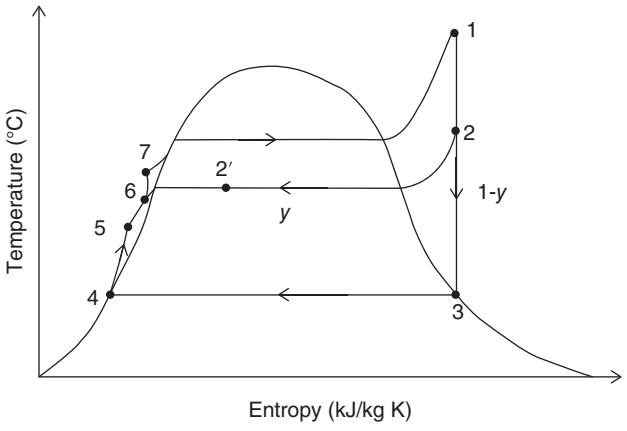

Figure 1.30 *T–s* diagram of the cogeneration Rankine cycle.

The overall efficiency of this thermodynamic cycle is given by:

$$\eta = \frac{|W_{turb}| + |E_{thermal}| - W_{pump1} - W_{pump2}}{Q_{in}} \tag{1.32}$$

$$\eta = \frac{h_1 - h_2 + (1-y)(h_2 - h_3) + y(h_2 - h_2') - (1-y)(h_5 - h_4) - (h_7 - h_6)}{h_1 - h_7}$$

where, h is the enthalpy at a certain point denoted by the number, W is the work done, $E_{thermal}$ is the thermal energy, and Q_{in} is the energy input.

Please note that the configuration shown in Figures 1.29 and 1.30 is just one possible configuration of the cogeneration Rankine cycle. Other configurations exist and each one is specific to a certain type of application. For example, Figure 1.31 is a cogeneration cycle used for hot temperature applications, where instead of extracting steam from the turbine at an intermediate pressure, the steam is extracted just after the boiler. Hence, this steam is hotter (because its pressure is higher) and for that reason the configuration is suitable for hot temperature applications. It is also controllable by means of an expansion valve positioned just before the heat exchanger which controls the pressure (and therefore the temperature) inside the exchanger allowing the system to adapt to different heating demands.

1.2.5 Other Configurations of the Rankine Cycle

So far, only the classical Rankine cycle and its possible improvements have been presented. This section now describes other thermodynamic cycles, derived from the Rankine cycle, which also use steam as a working fluid.

1.2.5.1 Supercritical Rankine Cycles

As we have noted previously, increasing the HP of the system results in a more work given to the turbine. However, because of the vapour dome, it also results in a lower steam quality at the end of the expansion phase. The supercritical Rankine cycle

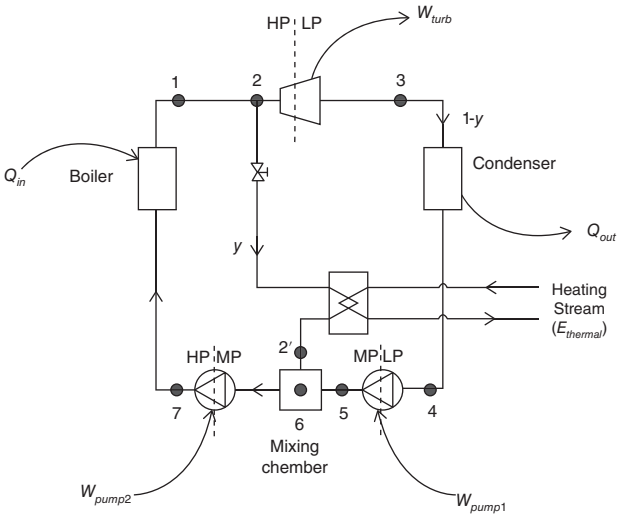

Figure 1.31 Schematic of a cogeneration Rankine cycle for hot temperature applications.

(SRC) bypasses this issue, because the working fluid is brought to such a condition that its pressure is above its critical pressure – a condition where the fluid is in a *supercritical* state and where there is now no longer a link between its vapour pressure and its temperature.

Advances in metallurgy and manufacturing techniques have made this possible, to the point where we can realistically increase the HP to a pressure greater than the critical pressure (for water) of 22.064 MPa (220.64 bar).

Hence, in an SRC, as the name implies, the fluid is in a supercritical state, i.e. it is behaving as a liquid and a gas at the same time. Working as a SRC increases the area of the cycle on the *T*–*s* diagram (see Figure 1.32), with a resultant increase in the work given by the fluid to the turbine.

As their working fluid, SRCs can use steam or organic fluids, but steam is still the most common fluid for both nuclear and fossil fuel power plants.

1.2.5.2 Reverse Rankine Cycles

The reverse Rankine cycle is another Rankine cycle widely used in the refrigeration sector, where instead of cycling clockwise on the *T*–*s* diagram, the cycle operates in a counterclockwise direction (as shown in Figure 1.33).

As we might expect, the components involved in this cycle are different and comprise:

- A compressor, used to compress the gas
- A condenser, used to cool and liquefy the fluid
- An expansion valve, used to drop the pressure of the liquid and so expand it back to a gas
- An evaporator, used to take heat from the environment

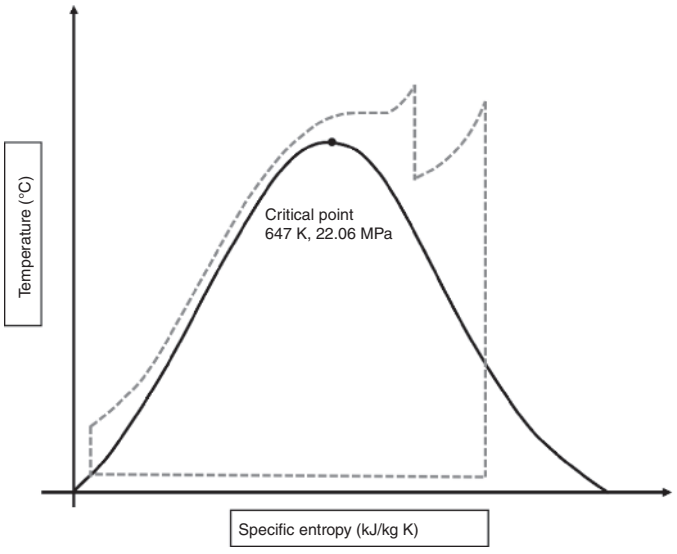

Figure 1.32 *T–s* diagram of a supercritical Rankine cycle using water as a working fluid.

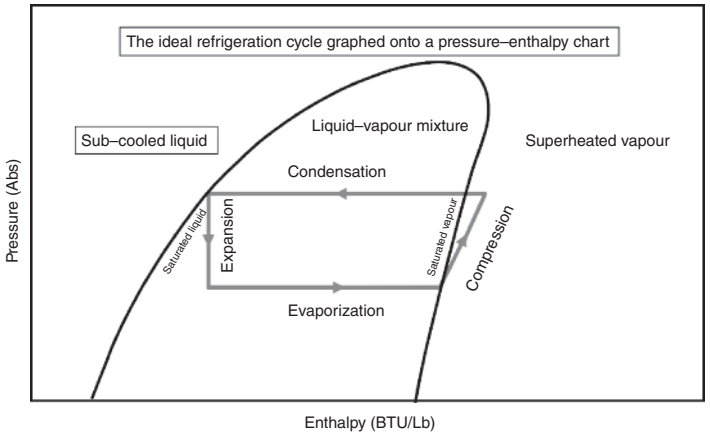

Figure 1.33 *P–V* diagram of the reverse Rankine cycle.

1.2.6 Rankine Cycles in Power Plants

The main application of the Rankine cycle is in converting thermal energy into mechanical energy in order to then obtain electrical energy. Hence, Rankine cycles are used in almost every high-temperature thermal power plant (fossil fuel, nuclear, geothermal, biomass, concentrated solar power, etc.). This section briefly showcases these different kinds of thermal power plant and their associated Rankine cycle.

1.2.6.1 Fossil Fuel Power Plants

Fossil fuel power plants consume either coal, fuel, or natural gas; the output power of such power plants typically range between 500 and 700 MW. The operation of

such plant is based on complex Rankine cycles involving several turbines, pumps, reheaters, and regenerators, and sometimes, multiple thermodynamic cycles are used to improve the overall efficiency of the power plant. For example, the CCGT is a type of power plant using natural gas as fuel, which uses both the Rankine cycle and a gas turbine (Brayton) cycle to rotate two different electric generators.

In most cases, the cycle working fluid is still water because the temperature of the hot source is high enough to vapourise the fluid under HP conditions.

1.2.6.2 Nuclear Power Plants

Enriched uranium is a high-energy density fuel – producing 1000 kWh requires only 4 g of this material whereas it requires 350 kg of coal! The power output of a nuclear reactor is often between 0.9 and 1.5 GW [13] and different designs of nuclear reactor exist, the most widespread being light water reactors such as the EPR reactor or the AP1000 reactor. Heavy water, gas-cooled, and fast neutron reactors are less common but provide other advantages over light water reactors [14].

In light water reactors, three water circuits are used to avoid radiation contamination. The primary circuit is still a hot water loop and is the hot source for the second circuit, which then operates through a complex Rankine cycle. The third circuit is used in order to cool the fluid after the expansion phase and acts as a condenser.

1.2.6.3 Overall Efficiency of a Power Plant

To determine the best way to convert energy into electricity we can compare the overall efficiencies for different types of power plants. The overall efficiency of a power plant corresponding to the ratio between the thermal energy input and the electrical energy output over a given time being:

$$\eta_{overall} = \frac{\text{Electrical energy provided by the plant}}{\text{Thermal energy given by the combustible}} \tag{1.33}$$

For the fossil fuel power plants, the thermal energy given by the combustible corresponds to the heat of combustion for the mass of fuel used during the given time, and the current average value of the efficiency of a Rankine-based power plant using fossil fuel is 33% [15]; however, it can range up to 40% in some cases [16]. In comparison, CCGT power plants have an average efficiency of 45% but they can reach values in excess of 50% and the efficiencies of current nuclear power plants are similar to the efficiencies of the Rankine-based fossil fuel power plants, i.e. with an average value of 33%.

Figure 1.34 is an illustration of the losses occurring during the energy transformation process:

- Neither the combustion of the fluid nor the nuclear fission reaction are perfect processes. Hence it is necessary to introduce a boiler efficiency term (η_{boiler}) to quantify the amount of heat given to the system compared to the heat delivered by the combustible/reaction:

$$\eta_{boiler} = \frac{Q_{in}}{\text{Thermal energy given by the combustible}} \tag{1.34}$$

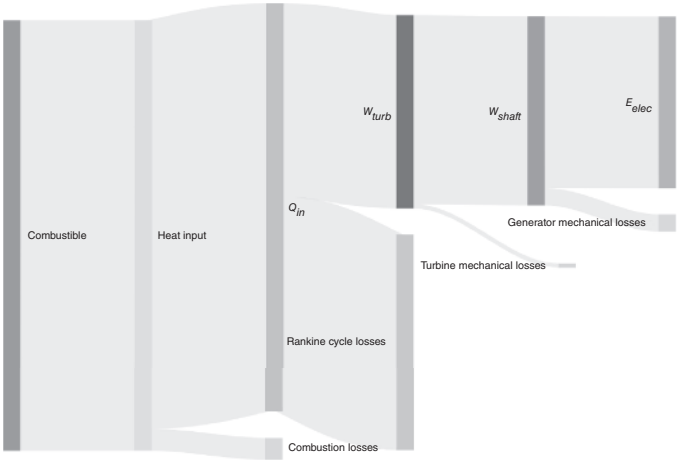

Figure 1.34 Sankey diagram of a Rankine-based power plant.

- The efficiency of the Rankine cycle (Eq. (1.14)) always induces energy losses. Indeed, even if the cycle was ideal and without irreversibilities, some losses would still be introduced by the cycle because the efficiency of this cycle cannot be higher than the Carnot's efficiency (Eq. (1.5)).
- Some of the work given by the fluid to the turbine is dissipated because of the turbine mechanical efficiency:

$$\eta_{turb} = \frac{W_{shaft}}{W_{turbine}} \tag{1.35}$$

- Finally, the generator does not convert 100% of the mechanical energy to electrical energy:

$$\eta_{generator} = \frac{E_{elec}}{W_{shaft}} \tag{1.36}$$

So, in the end and assuming the pumps of the system are powered by the plant itself, this leads to an overall efficiency equation for the power plant of [17]:

$$\eta_{overall} = \eta_{boiler} \cdot \eta_{actual\ cycle} \cdot \eta_{turb} \cdot \eta_{generator} \tag{1.37}$$

Of course, this 'overall' efficiency only takes into consideration the losses occurring during the production of the electrical power. It should also be noted that there are many other sources of loss that occur after this production phase, e.g. during the transport (transmission and distribution) phase and the consumption phase.

1.2.6.4 Case Studies

We need to appreciate that whilst real steam power plants are based on the Rankine cycle, they used very complex configurations of this thermodynamic cycle, involving a lot of components, in order to reach the maximum efficiency for a reasonable economic investment [18].

In these power plants, reheating and regeneration processes are widespread.

For instance, a combination of turbines are used as well as FWHs – all of them working under different pressure conditions. Among these only one is an open FWH, the others are closed FWHs using the drain cascaded backward technology. Pumps are not included on this diagram but, for this configuration, at least four pumps are necessary to increase the pressure of the fluid from one pressure stage to the next. Of course, to control this system, a lot of valves, sensors, and controllers are also required. So, when compared to the classical ideal Rankine cycle, this power plant cycle is very much more complex.

The overall efficiency of a steam power plant thermodynamic cycle is given by:

$$\eta = \frac{\Sigma|W_{turb}| + \Sigma|E_{thermal}| - \Sigma W_{pump}}{\Sigma Q_{in}} \tag{1.38}$$

1.3 Organic Rankine Cycle

The organic Rankine cycle (ORC) is very similar to the Rankine cycle, the prefix 'organic' being derived from the fact that ORC devices use organic compounds rather than water as their working fluid. Interest in ORC has accelerated in the past 10 years, particularly in the areas of waste heat recovery and renewable energy generation.

The typical parts found in an ORC are not dissimilar from those found in conventional Rankine cycle plant and these include:

1. Pump
2. Evaporator
3. Expansion device
4. Condenser

The devices are constructed to form a circuit in the order of the list provided earlier, however the configuration of an ORC system can vary depending on its application. Further stages such as preheating and regeneration may also be included to both improve the efficiency and also help by recovering energy from other sources. Furthermore, different working fluids also affect the performance of an ORC, with the selection of the working fluid being largely determined by its application, and where the temperature of the target heat source is highly influential. To analyse such systems, we need to note:

Mass conservation is governed by the following equation:

$$\sum \dot{m}_{out} = \sum \dot{m}_{in} \tag{1.39}$$

where $\dot{m}_{out}$ (kg/s) is the mass flow rate of working fluid out of the closed system, and $\dot{m}_{in}$ (kg/s) is the mass flow rate into the closed system.

The heat flow between any two points are defined using the following equation:

$$\dot{Q} = \dot{m} \cdot \Delta h \tag{1.40}$$

where $\dot{Q}$ (kW) is the heat flow, $\dot{m}$ (kg/s) is the mass flow rate, and Δh is (kJ/kg) the difference in enthalpy between two points in the ORC.

So, the net mechanical work is described using the following equations:

$$\dot{W}_{out} = \dot{W}_{gross} - \dot{W}_{in} \tag{1.41}$$

$$\dot{W}_{out} = \dot{m} \cdot \Delta h_{exp} \tag{1.42}$$

where $\dot{W}_{out}$ (kW) is the net mechanical power output from the ORC system, $\dot{W}_{gross}$ (kW) is the gross mechanical power output from the ORC, $\dot{W}_{in}$ (kW) is the gross mechanical power input into the ORC and Δh_{exp} (kJ/kg) is the enthalpy change across the expansion device.

Since the only input considered in the configurations is the pump, $\dot{W}_{in}$ can be calculated using Eq. (1.43).

$$\dot{W}_{in} = \frac{\dot{m}}{\rho} \cdot P \tag{1.43}$$

where $\dot{m}$ (kg/s) is the mass flow rate, ρ (kg/m) is the density of the working fluid under the working conditions, and P (N/m)] is the pressure.

1.3.1 Configurations of ORC

Like the Rankine cycle, the ORC exists in many different configurations each one of which has advantages and drawbacks and so is only suitable for a specific application.

1.3.1.1 Basic ORC Configuration

The basic configuration of an ORC is laid out in Figure 1.35; the system receiving and producing useful energy from one heat source, and Figure 1.36 shows the *T*–*S* graph for the same.

The evaporator between 2 and 3 heats the working fluid until it boils, and during boiling, although the temperature remains constant, the entropy increases. This boiling is represented by the flat line on the *T*–*S* graph. In the expander (between 3 and 4) the gaseous working fluid undergoes expansion where its temperature decreases. Finally, between 4 and 1 the working fluid passes through a condenser where the fluid returns to the liquid state ready for the process to begin again.

The equations governing the basic ORC are given subsequently.

$$\dot{Q}_{eva} = \dot{m} \cdot (h_3 - h_2) \tag{1.44}$$

$$\dot{W}_{exp} = \dot{m} \cdot (h_3 - h_4) \tag{1.45}$$

$$\dot{W}_{pump} = \dot{W}_{in} \tag{1.46}$$

$$\eta_{exp} = \frac{\dot{W}_{exp}}{\dot{Q}_{eva}} \tag{1.47}$$

$$\eta_{basic} = \frac{\dot{W}_{exp} - \dot{W}_{pump}}{\dot{Q}_{eva}} \tag{1.48}$$

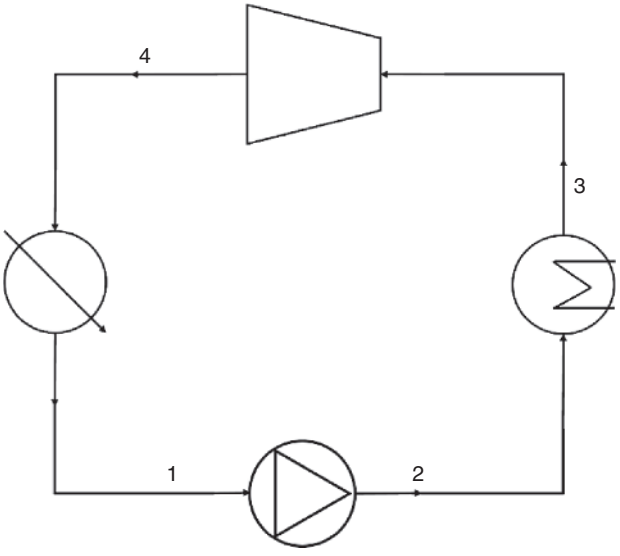

Figure 1.35 Schematic of a typical ORC device.

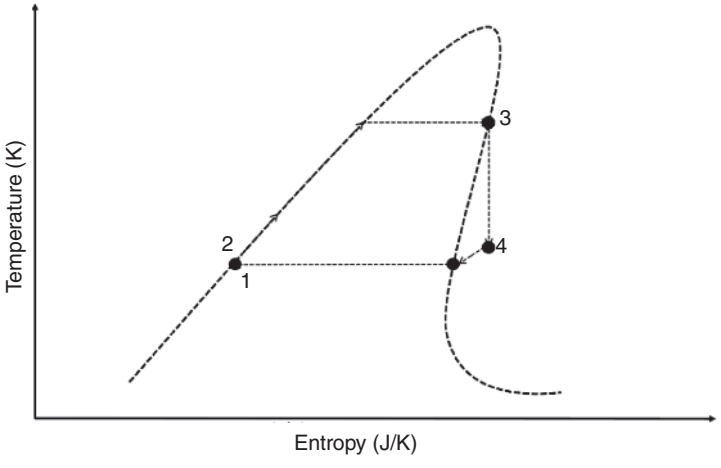

Figure 1.36 *T–S* graph of basic ORC system.

where η_{exp} is the efficiency of the expander in the recovery of energy from the evaporator (%) and η_{basic} is the thermal efficiency of the entire basic ORC configuration (%).

1.3.1.2 ORC with Preheating

Typically, configurations of ORC systems are more complicated where they are designed and constructed to recover energy from multiple heat sources.

In automotive applications, e.g. heat can be recovered from both the exhaust gases and the coolant liquid, so in this format the preheating system involves a heat

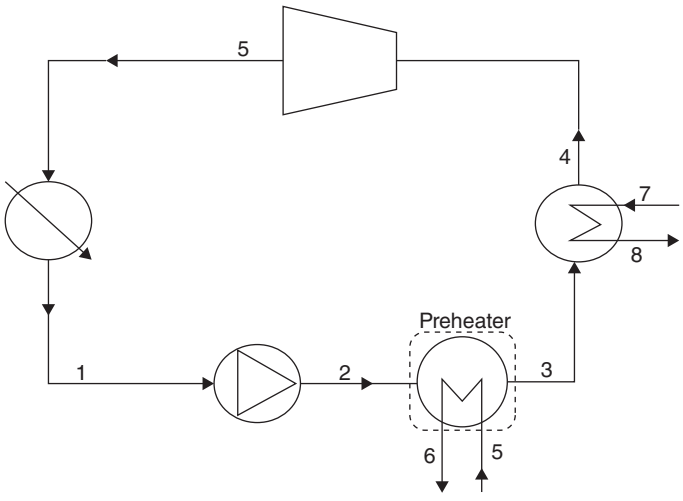

Figure 1.37 Schematic of an organic Rankine cycle with preheater.

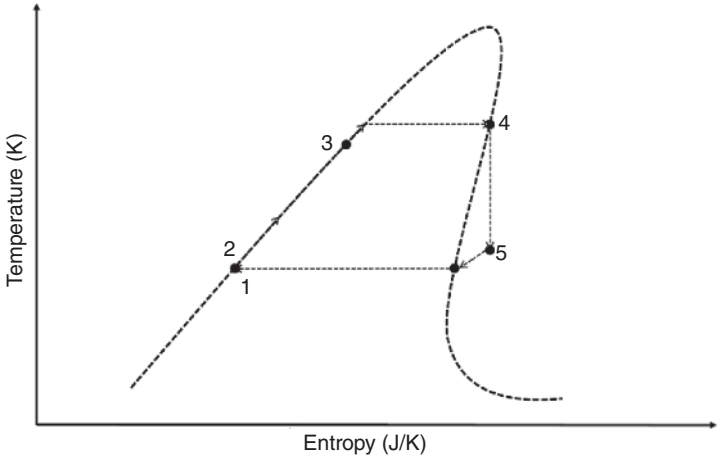

Figure 1.38 *T–S* graph of ORC system with preheater.

exchanger between the pump and the expansion device which then recovers heat energy from the engine coolant fluid and transfers it to the working fluid.

This is shown in Figure 1.37 – the preheater in this case increasing the energy content of the working fluid, so reducing the energy required for its evaporation in the evaporator. This process is represented in Figure 1.38 by the additional heating shown between 2 and 3, the preheating increasing the efficiency of the process by reducing the energy required in the evaporation for boiling to occur.

The equations governing the ORC with preheating are given subsequently.

$$\dot{Q}_{eva} = \dot{m}_{3-4} \cdot (h_4 - h_3) = \dot{m}_{7-8} \cdot (h_7 - h_8) \tag{1.49}$$

$$\dot{Q}_{pre} = \dot{m}_{2-3} \cdot (h_3 - h_2) = \dot{m}_{5-6} \cdot (h_5 - h_6) \tag{1.50}$$

$$\dot{W}_{exp} = \dot{m} \cdot (h_4 - h_5) \tag{1.51}$$

$$\dot{W}_{pump} = \dot{W}_{in} \tag{1.52}$$

$$\eta_{exp} = \frac{\dot{W}_{exp}}{\dot{Q}_{eva} + \dot{Q}_{pre}} \tag{1.53}$$

$$\eta_{pre} = \frac{\dot{W}_{exp} - \dot{W}_{pump}}{\dot{Q}_{eva} + \dot{Q}_{pre}} \tag{1.54}$$

1.3.1.3 Recuperative ORC

In order to improve the overall thermal performances of the system, preheating of the working fluid can also be achieved by recuperation as shown in Figure 1.39. As with normal preheating, this process impacts the working fluid both before the evaporator but unlike normal preheating, it also affects the working fluid after the evaporator, and these effects are shown between points 2 and 3 and 5 and 6 on Figure 1.40. As with preheating, the process reduces the energy needed for boiling to occur in the evaporator.

The equations governing the recuperative ORC are given subsequently.

$$\dot{Q}_{eva} = \dot{m} \cdot (h_4 - h_3) \tag{1.55}$$

$$\dot{Q}_{rec} = \dot{m} \cdot (h_3 - h_2) \tag{1.56}$$

$$\dot{W}_{exp} = \dot{m} \cdot (h_4 - h_5) \tag{1.57}$$

$$\dot{W}_{pump} = \dot{W}_{in} \tag{1.58}$$

$$\eta_{expansion} = \frac{\dot{W}_{exp}}{\dot{Q}_{eva} + \dot{Q}_{rec}} \tag{1.59}$$

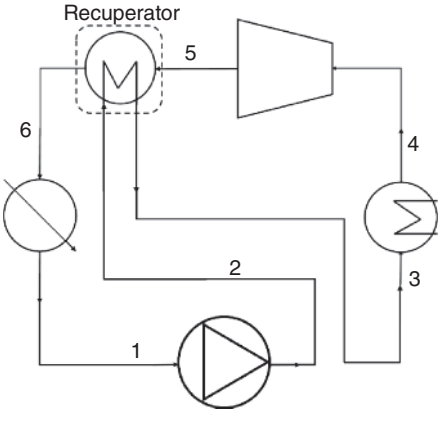

Figure 1.39 Schematic of an organic Rankine Cycle with recuperator.

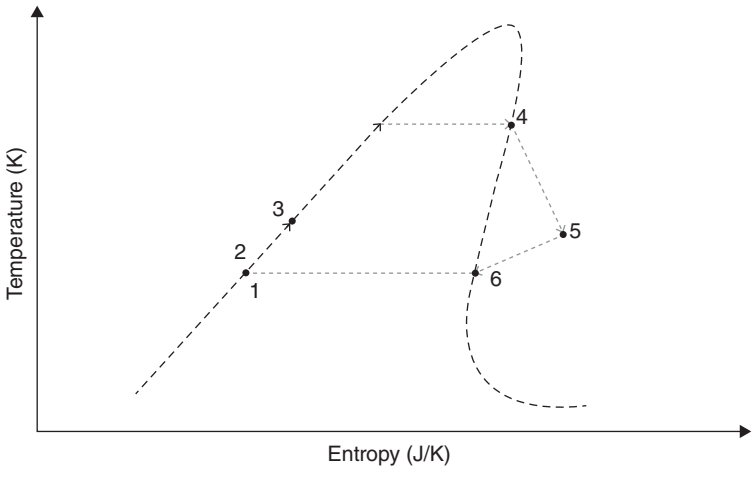

Figure 1.40 *T–S* graph of ORC system with recuperator.

$$\eta_{net} = \frac{\dot{W}_{exp} - \dot{W}_{pump}}{\dot{Q}_{eva} + \dot{Q}_{rec}} \tag{1.60}$$

1.3.1.4 Recuperative ORC with Preheating

In fact, both preheating and recuperation can be combined and operated within the same system and this is shown in Figure 1.41. This is a combination of both the processes that were shown in Figures 1.38 and 1.40; the entire process being described by the *T–S* graph in Figure 1.42 where recuperation and preheating reduce the energy required for boiling the fluid within the evaporator and also assist in the condensation process of the working fluid after the expansion device.

The equations governing the recuperative ORC with preheating are given subsequently.

$$\dot{Q}_{eva} = \dot{m} \cdot (h_5 - h_4) \tag{1.61}$$

$$\dot{Q}_{rec} = \dot{m}_{2-3} \cdot (h_3 - h_2) \tag{1.62}$$

$$\dot{Q}_{pre} = \dot{m} \cdot (h_4 - h_3) \tag{1.63}$$

$$\dot{W}_{exp} = \dot{m} \cdot (h_4 - h_5) \tag{1.64}$$

$$\dot{W}_{pump} = \dot{W}_{in} \tag{1.65}$$

$$\eta_{exp} = \frac{\dot{W}_{exp}}{\dot{Q}_{eva} + \dot{Q}_{rec} + \dot{Q}_{pre}} \tag{1.66}$$

$$\eta_{pre} = \frac{\dot{W}_{exp} - \dot{W}_{pump}}{\dot{Q}_{eva} + \dot{Q}_{rec} + \dot{Q}_{pre}} \tag{1.67}$$

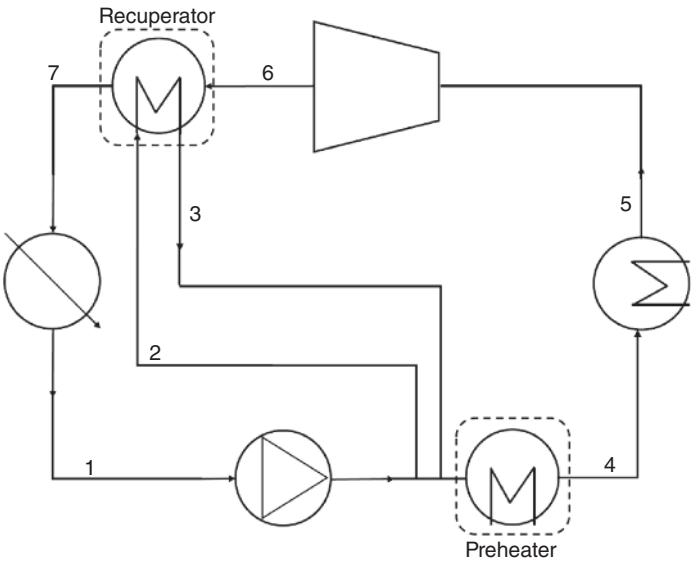

Figure 1.41 Schematic of an organic Rankine cycle with preheater and recuperator.

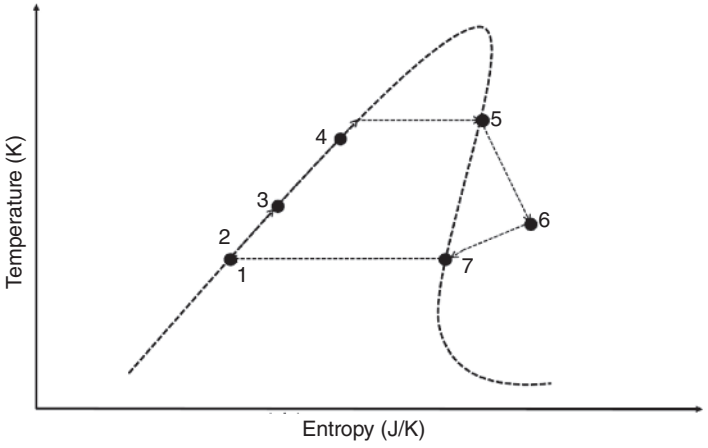

Figure 1.42 *T–S* graph of ORC system with recuperator and preheater.

1.3.2 Organic Working Fluids

Many different working fluids are used in ORC systems and the choice is largely determined by the conditions under which the system is designed to operate. Organic working fluids not only behave differently to water they each also have different characteristics, but these can be split into three categories known as: dry-, isentropic-, and wet-type working fluids. Wet, isentropic, and dry working fluids have $\frac{dT}{dS}$ values of <0, ∞, and >0 respectively, and the *T–S* graphs are displayed in Figures 1.43–1.45, respectively.

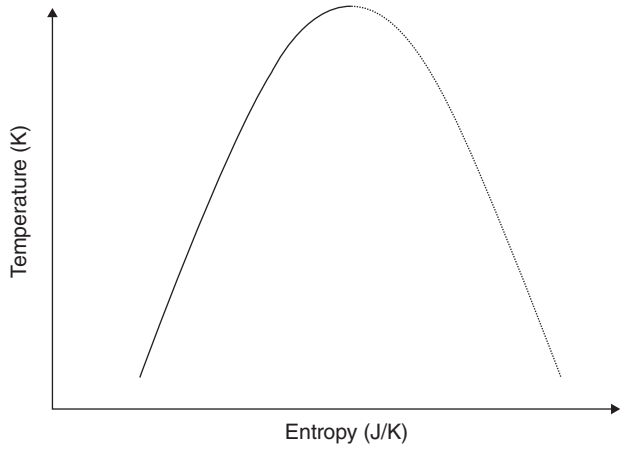

Figure 1.43 *T–S* diagram of a wet-type working fluid.

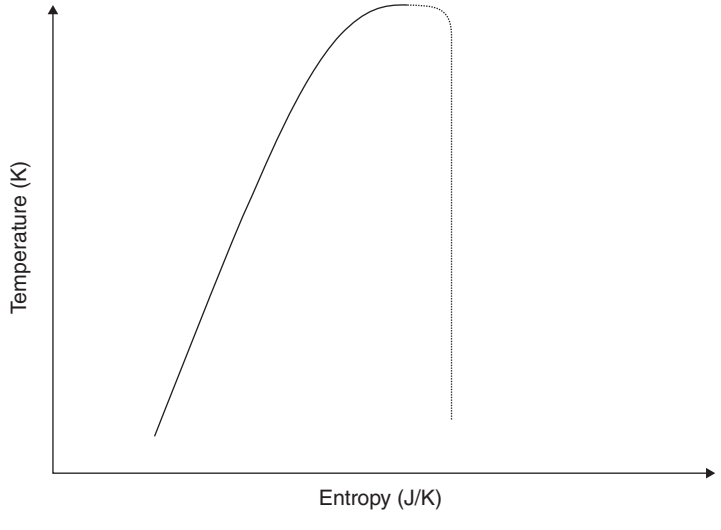

Figure 1.44 *T–S* diagram of an isentropic-type working fluid.

There are four major benefits of using organic working fluids over water in Rankine cycles:

1. *Less heat is required for evaporation*: This can be seen as the width of the *T–S* curve is narrower for dry and isentropic working fluids than for wet working fluids.
2. *Evaporation occurs at lower temperatures and pressures than water*: The reduced temperature of evaporation means that organic working fluids can be used to recover energy from lower temperature heat sources than conventional Rankine cycles.
3. *Outlet from expansion devices is a vapour at lower temperatures*: This reduces the likelihood of damage to the expansion device, because condensation should only

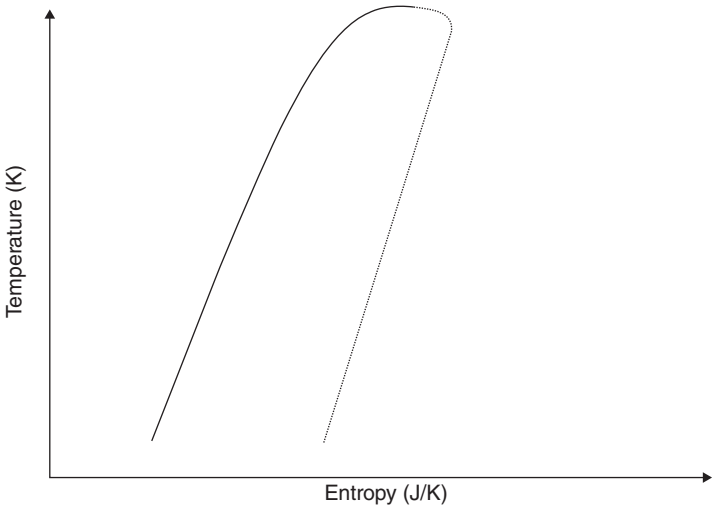

Figure 1.45 *T–S* diagram of a dry working fluid type.

occur after expansion. However, when the expansion inlet temperature is low and the inlet pressure is high, because wet organic working fluids have lower efficiencies than other working fluids they may start to condense within the expansion device potentially causing damage. This is one reason why dry and isentropic working fluids are more popular in ORC systems, where after isentropic expansion, they exist in the superheated state, reducing the risk of condensation and thus minimising potential damage to the expansion device [19].

4. *Smaller temperature difference between evaporation and condensation*: This results in reduced pressure drop across the condenser.

1.3.3 Organic Working Fluid Selection

The selection of the correct working fluid is critical to optimising the efficiency of an ORC system. As such, it is one if not *the* most important aspect of an ORC design. Working fluids are chosen based on their environmental sustainability, ozone depletion, global warming potential (GWP), safety including flammability, toxicity, and corrosivity, boiler vapour pressure, critical temperature, and thermal stability as shown in Table 1.1 [20].

These characteristics affect the behaviour of the fluids upon heating – as seen in the *T–s* graph for different working fluids in Figure 1.46 – and so under specified conditions, there should be a specific working fluid that will result in optimum ORC energy recovery. However, we should also note that certain conditions such as high temperatures and pressures make the use of some organic working fluids unsafe.

As discussed already, if the temperature in the evaporator is low, then the working fluid may condense within the expansion device resulting in decreased efficiency and possible damage. Additionally, any working fluid that requires more entropy to

Table 1.1 Basic properties of working fluids.

Fluid	Critical temperature (°C)	Critical pressure (kPa)	Density at 25 °C (kg/m^3)	Heat of vapourisation at 1 bar (kJ/kg)
R134a	101	4059	4.258	217
R227ea	102.8	2999	7.148	131.7
R245fa	154	3651	5.718	196
R123	183.68	3668	1464	170.6
R600	151.98	3796	2.441	358
Toluene	318.6	4126	862.2	361.3
iso-Butane	134.7	3640	2.44	165.5
iso-Pentane	187.2	3370	614.5	342.5
n-pentane	196.5	3364	620.8	358

Source: Table from Darvish et al. [20].

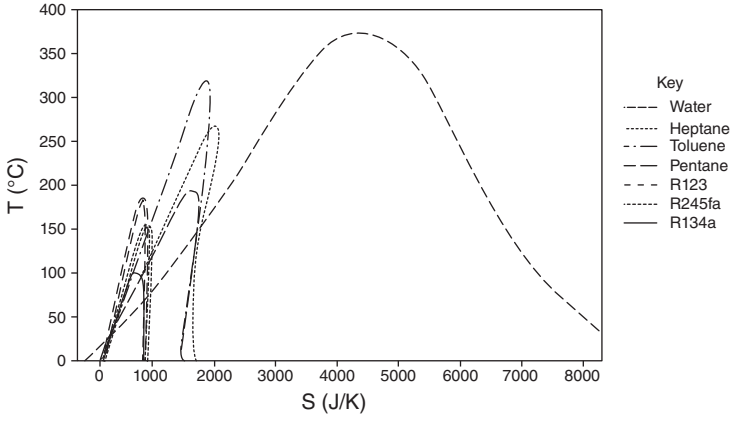

Figure 1.46 *T–S* diagram for different working fluids.

reach the superheated phase then also requires longer exposure within the evaporator, and this would result in a lower mass flow rate than selecting a different working fluid that requires less entropy to reach the superheated phase.

Different temperature–pressure charts are shown in Figure 1.47 for various common working fluids. This figure shows that different working fluids exist at different pressures under the same temperature; these pressure differences also increase with temperature. Choosing an incorrect working fluid could therefore present a safety issue – where pressures increase with temperature, then they exceed the safe limits of the system, resulting in its failure. Under such circumstances, a higher flow rate would be required in order to reduce the risk of this safety issues and such a pump

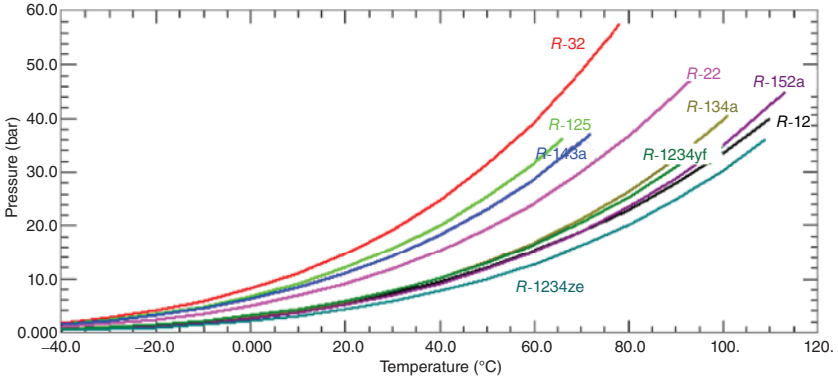

Figure 1.47 Temperature–pressure charts for different working fluids. Source: Abas et al. [21].

would require a higher energy input – potentially resulting in decreased system efficiency. The selection of the correct working fluid therefore is essential to ensure the safety and high efficiency of an ORC system.

These examples – extreme as they may seem – indicate in terms of both efficiency and safety the importance of selecting the correct organic working fluid for an ORC waste heat recovery system.

Although not always the case historically, in addition to system safety issues, working fluids are now also selected on their sustainability. In the past, organic working fluids included chlorofluorocarbons (CFCs), which due to their high ozone depletion potentials (ODPs) were subsequently banned, and working fluids were developed that had significantly smaller ozone reduction potentials. Nonetheless, despite the benefits of reduced ozone depletion capacity, these improved fluids still possessed very high GWPs and so, in turn, this then has led to the development of working fluids with reduced GWPs such as R123 and R600. The ozone depletion and GWPs of some common working fluids are shown in Table 1.2.

Note: ODP is defined as the relative amount of degradation to the ozone layer a substance can cause, with trichlorofluoromethane (R-11 or CFC-11) being fixed at 1.0.

Table 1.2 Sustainability aspects of some common working fluids.

Fluid	Ozone depletion potential	Global warming potential (equivalent CO_2)	Sources
R134a	0	1300	[22]
R227ea	0	3220	[23]
R245fa	0	1030	[24]
R123	0.02	0.02	[22]
R600	0	3	[25]

Table 1.3 Table showing typical applications of ORC in the industry.

Description/ working fluid	Focus	Industry	Temperature of source (°C)	Sources
Sewage heat recovery TY-1	Sustainability of system	Petrochemical industry	110	[26]
Heat recovery from feeder ship engine	Reducing NO_x and SO gases in exhaust emissions	Shipping	450	[27]
Heat recovery from car exhaust gas under different conditions	Energy recovery under three different ambient conditions, and different engine operating conditions	Automotive	500	[28]

1.3.4 Applications of the ORC

There are two main energy applications for the ORC: one is waste heat recovery (where ORC is used to improve the performance of an energy production process or recover energy from an exhaust stream) and the other being in the renewable energy sector. Here ORCs can be used to recover energy from geothermal energy, solar energy, and biomass combustion.

1.3.4.1 Waste Heat Recovery

The ORC is typically used for power output range between 100 kW and 2 MW, and Table 1.3 shows some example applications of ORC, typically in recovery of waste heat from exhaust gases in the industries identified. Configurations of the ORC can also vary depending on the application.

Renewable Energy

Biomass: Biomass energy generation is becoming more popular as it is now quite possible to produce energy from food waste and other organic materials that historically would be seen as waste materials. Furthermore, biomass fuels can be reproduced more quickly than fossil fuels – the length of the carbon cycle being much shorter for biomass than for fossil fuels. Unfortunately for this application, biomass fuels typically burn at lower temperatures than fossil fuels. Which means that conventional Rankine cycles are exposed to a higher risk of condensation within the expanders when used for power generation and biomass boilers. Consequently, conventional Rankine cycles may require superheating to allow their use in biomass energy recovery, and for this reason, ORCs are a popular energy recovery solution for use with biomass fuels [29].

Solar: ORCs make possible the recovery of thermal energy from solar radiation particularly in warmer countries. The low boiling temperatures of the organic

working fluids used allows for the capture of energy from the Sun in such devices as flat panel collectors. Phase change materials can also be incorporated into such systems to store heat when energy is not required or when excess energy is being produced, this stored energy then being released later [30].

Geothermal: Ground source heat pumps allow for the cooling or heating of a property making use of the soil and rock as an energy store. This is practical because the year-round temperature of soil and rock at depths of only a few metres is assumed to be constant. Therefore, in summer, heat pumps can be used in reverse to take thermal energy from the air within a building and store it in the ground; whilst in winter, the process can be reversed, and energy taken from the ground can be used to heat the air inside the building. These systems can be improved by the use of ORC systems that help solve the 'cold accumulation problem' of such systems, by storing energy in seasons that require less heating [31].

1.4 Kalina Cycle

The Kalina cycles are a family of thermodynamic power cycles that utilise a mixture of fluids as their working fluid. The first Kalina cycle (also sometimes called the *reverse absorption* cycle) was developed in 1984 by Alexander Kalina, a Russian engineer [32], who then founded Exergy Inc., a company specialising in energetic efficiency and waste heat recovery.

The family of cycles was still inspired by the family of Rankine cycles. Their main goal being to further improve both the energetic and exegetic efficiencies of the thermodynamic power cycle by making use of the fact that in Rankine cycles a lot of energy is lost during the boiling phase. Moreover, as the temperature profiles of the working fluid and the heating fluid do not match the thermal behaviours of the source and working fluid diverge, thus irreversibilities are created and exergy is destroyed. Kalina cycles therefore offer a solution to this energetic issue and represent a big step forward for power cycles and their use in electricity generation [33].

In this section, the theoretical operation of Kalina cycles will be explained and illustrated. The advantages and drawbacks of this new family of power cycle are also discussed and compared to both classical steam cycles and ORCs. Next, applications for these thermodynamic cycles are presented and some case studies are used to clarify explanations. Lastly, current researches on Kalina cycles are briefly reviewed to give the reader an indication of the current state of research on this subject.

1.4.1 Cycle Fundamentals

As just stated, the Kalina cycle is a power cycle based on the Rankine cycle. The difference arises in using a mixture of fluids as the working fluid.

Using a mixture of fluids (instead of a pure substance) as the working fluid allows vapourisation and condensation to occur under a constant pressure through a

non-isothermal process. This kind of mixture being called a non-azeotropic mixture (one with components that have different boiling points), as this way there is a better match between the temperature profiles of the working fluid and the heating fluid during the boiling phase. Helpfully, this is also the case between the working fluid and the cooling fluid in the condensation phase.

Currently, the most commonly used mixture for a Kalina cycle is an ammonia–water solution, and although relatively new, this mixture has proven its efficiency through various experiments and pilot projects [33].

It is successful because in a Kalina cycle, the mass fraction of ammonia has a new degree of freedom, allowing more flexibility and so reaching higher efficiencies. The main feature being that the mass fraction of ammonia is now directly linked to the saturation pressure of the mixture. So if, e.g. the pressure is held constant whilst the mass fraction of ammonia is decreasing, then vapourisation of the fluid will start at a higher temperature, as shown in Figure 1.48.

The ammonia vaporises first because it is more volatile than water and hence the mixture concentration of ammonia decreases, and this leads to an increase of the saturation temperature of the resultant mixture. This way, the boiling phase occurs over a range of temperatures and not just at one given temperature as would be the case for a pure substance.

Being able to control the mass fraction of ammonia in each part of the circuit is therefore an important factor and so, in comparison to more conventional steam cycles, Kalina cycles require new components. For example, a separator is certainly required to control the proportion of ammonia in the mixture. This control must occur at every stage of the circuit, so within the separator are two different phases: a liquid phase which is a lean ammonia–water solution (as ammonia is more volatile than water) and a gas phase which is rich in ammonia. Mixing one of these phases with the working ammonia–water solution is a way to either increase or decrease the mass fraction of the ammonia depending on which phase is being mixed with the solution.

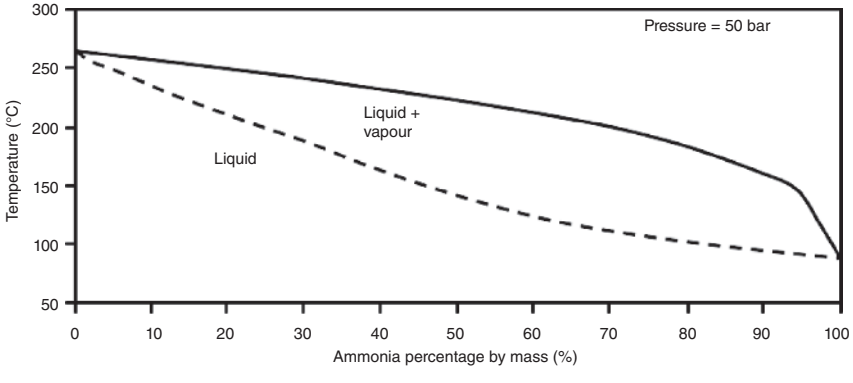

Figure 1.48 Saturation temperature as a function of ammonia concentration for an ammonia–water solution at a pressure of 50 bar.

To operate correctly, a high proportion of ammonia is required in the boiler to enhance the heat transfer. However, keeping this high proportion of ammonia during the condensation phase implies a very low condensation temperature or pressure. So, to overcome this issue, the concentration of ammonia in the ammonia–water solution is reduced before the condensation phase. It was used to demonstrate the feasibility of the Kalina cycles in Canoga, New York, in 1992 on a 6.5 MW power plant [34].

In this configuration, the boiler of the system is also called the *heat recovery vapour generator* (HRVG). Moreover, the subsystem operating the condensation and distillation phase is called *distillation and condensation subsystem* (DCSS). Those two acronyms are widely used for Kalina cycles. Throughout the cycle, the ammonia concentration of the mixture is varying. It is like different fluids were being used, i.e. the fluid in the boiler section is very different from the fluid in the condenser section. Many other configurations also exist, each tailored for a specific application.

1.4.1.1 Why Use Ammonia–Water Solution in Kalina Cycle?

At this time, Kalina cycles predominantly use the ammonia–water solution with hardly any other variants being reported. The mixture displays interesting physical, chemical, economic, and ecological properties, and by varying the percentage mix it can be made to behave like different fluids compared to a pure compound. The main reason therefore for choosing this solution is its flexibility, since by varying the ammonia concentration using distillation, we can alter either the temperature or the pressure of saturation.

Ammonia–water solution also has an excellent heat transfer coefficient and a low freezing point. In addition, because ammonia and water have similar molecular weights, it is possible to use standard components (turbine, pump, etc.) that have already proven their efficiencies in steam power plants. However, some materials such as copper, aluminium, and mild steel cannot be used with ammonia, but otherwise standard materials such as carbon steel and standard high-temperature alloys are fine.

In addition, from an economic point of view, the two components of the mixture are relatively inexpensive and widely available. Water is abundant and ammonia is produced on a world-scale for industrial and domestic uses.

The main issue with ammonia is its toxicity. If the human brain is exposed to high levels of this substance, it can lead to drowsiness and coma [35]. However, as ammonia is a gas under atmospheric pressure and temperature, it is relatively easy to vent off and so with the relevant safety procedures, already proven in industrial plants that use large quantities of ammonia, its use here is considered acceptable. Moreover, as ammonia has a strong smell, it is a self-alarming product which makes its detection easier.

However, the usage of ammonia can also lead to different types of corrosion, and these will be discussed in Section 1.4.2.

Contrary to the fluids used in ORCs, ammonia and water are ecological-friendly. Indeed, the GWP of each are zero, which means that the accidental release of those fluids into the atmosphere has no effect on the global warming. Conversely, the fluids

used in ORCs have a proven effect on the global warming. So, in case of leakage from an ORC power plant, large quantities of fluid, harmful to the environment, could be released into the atmosphere. This is not the case for Kalina cycle-based power plants and furthermore, as with the modern organic fluids used in ORCs, the ODP of ammonia is also equal to 0.

1.4.2 Advantages and Drawbacks

To evaluate the potential of this technology, it is important to compare it with the current and most commonly used power cycles of steam systems and ORCs.

1.4.2.1 Advantages

Generally, Kalina cycles have better energetic and exergetic performances than Rankine cycles or ORCs.

As a reference, the Carnot's efficiency is given by:

$$\eta = 1 - \frac{T_C}{T_H} \tag{1.68}$$

In this formula, T_H (K) is the average hot source temperature and T_C (K) is the average cold source temperature. So if we can increase the average hot temperature and at the same time lower the average cold temperature, then the efficiency of the thermodynamic cycle will be improved. Kalina cycles achieve this, compared to not only the theoretical Carnot cycle, but also the very practical Rankine cycles. So for that reason alone, Kalina cycles have a better energetic efficiency.

Moreover, during the boiling and condensing phases, because the temperature profile of the mixture has a better match to the temperature profile of the heating/cooling fluid, heat exchanges are enhanced for Kalina cycles compared to Rankine cycles. Less exergy is destroyed during the heat exchange phases for Kalina cycles so the irreversibilities of the process are reduced. Simulations have showed that the best work output given by a Kalina cycle is 20% to 24% higher than the equivalent from a dual pressure Rankine cycle [33].

Also, when using a geothermal spring, Kalina cycles can generate from 10% to 50% more power than classical steam systems (ORCs), particularly when the temperature of the source is below 200 °C [36]. When the hot source is at medium temperature, e.g. with waste heat recovery, the efficiency increase provided by the Kalina cycle against steam cycles is between 10% and 40% [37].

The gains are not just in simulations. During the Global CempPower conference in 2012 [38], M.D. Mirolli (formerly from Wasabi Energy) and Kevin Happ (FLSmidth) reported that the use of Kalina cycles for waste heat recovery in the cement industry can lead to a 15–25% improvement of the recovery compared to current technologies (ORCs).

As we have already noted, because the properties of the working fluid can be changed during the operation of the plant, Kalina cycle-based plant can adapt easily to hot and cold days by varying the proportion of ammonia – this flexibility then allows Kalina cycles to harness energy from a wider range of low to medium–high-temperature heat sources.

The fact also that standard components can be used to operate a Kalina cycle is an advantage as it increases the reliability of the potential new power plants, because even if they are using a relatively new technology, their operation is based on tried and tested efficiency-proven components.

1.4.2.2 Drawbacks

Ammonia is a toxic fluid, so even if it is easy to vent off under atmospheric pressure and self-alarming due to its smell, it is relatively dangerous to use on a large scale. However, some safety procedures exist, and for the moment no health issue linked to Kalina cycle-based power plants have been recorded. Compared to the hydrocarbons used in ORCs, ammonia is non-flammable and does not represent an explosion hazard.

General corrosion can also occur with this type of power plant due to the presence of water. However, as ammonia raises the pH level of the solution, the phenomenon is less important than in classical steam cycles. Indeed, a high pH and a low oxygen proportion can result in the growth of protective magnetite layers (Fe_3O_4) on tube surfaces, but generally, a good control of the water chemistry is needed to avoid issues linked to corrosion.

The CO_2 level must also be controlled to avoid the formation of ammonium carbamate. This can occur if ammonia and carbon dioxide react under conditions of HP and high temperature. Furthermore, if the temperature of the mixture exceeds 400 °C, then ammonia becomes unstable and leading to nitride corrosion [39].

Currently, the physical properties of an ammonia–water solution are not yet fully known, particularly in the supercritical region where very little data is currently available. Some correlations exist and these are leading to smaller and smaller differences between experimental tests and simulations.

Kalina cycles are sometimes said to be more complex than steam cycles. This assumption is questionable, but it is undeniable that steam cycles have proved their efficiency and reliability across time. So even though pilot projects exist for the Kalina cycle it is relatively understandable why some industries are quite hostile to any additional investment in this technology at the present time.

1.4.3 Applications of the Kalina Cycle

Because the boiling temperature of the mixture varies, it can start to evaporate at a lower temperature than for the Rankine cycle at a given pressure. This is why Kalina cycles are mostly used in geothermal power plants (100–120 °C) and waste heat recovery (300–400 °C) [40]. For waste heat recovery applications, the most suitable applications are the cement industry, glass industry, petrochemical industry, steel industry, and potentially, for thermal power plants [39]. Using Kalina cycles as bottoming cycles in thermal power plant is possible, but for now it is not yet economically viable because the architecture of such a cycle is quite complex. Kalina cycles can also be used with alternative renewable energies other than geothermal, and some configurations of the cycle are made for solar thermal and ocean thermal [41] operations (Figure 1.49).

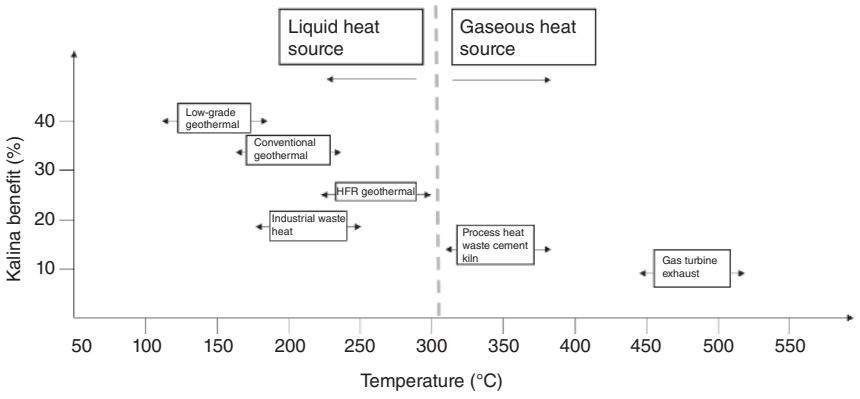

Figure 1.49 Kalina benefit as a function of heat temperature and types of applications.

1.4.3.1 The Different Configurations of the Cycle

Kalina cycles are part of a thermodynamic family of cycles. These vary by the number of each component, how they are arranged, and how they are linked together. To date, a lot of interesting Kalina cycle configurations have been designed and studied; every configuration being suitable for a particular type of application and so designated by a code. For example, KCS-1 was the very first cycle that used a mixture of fluids and was proposed by Kalina himself in 1984 [42].

All these thermodynamic cycles are split into two groups. The oldest ones are called *first-generation* Kalina cycles – the Kalina cycle being a trademark involving all the first-generation Kalina cycles [43].

Figure 1.50 shows three configurations of the Kalina cycle system [44], all suitable for geothermal applications. KCS-11 was designed for the high-temperature geothermal resources and KCS-34 for lower temperature geothermal resources. Those two cycles are the most common Kalina cycles used for geothermal application. KSG-1 is very similar to KCS-34, the KSG-1 patent is held by Siemens.

A second generation of Kalina cycle was developed by Dr. Alexander Kalina from 2008 to 2014. The patents for those new cycles are all owned by a company called Kalex LLC, founded by Kalina.

Those new cycles are more efficient and provide an improved power output. For example, the SG-2a cycle offers a better energetic and exergetic efficiency than either KCS-11 or KCS-34 when using geothermal heat sources in temperature range from 125 to 150 °C [45].

So even though these new cycles have a more complex architecture than their first-generation counterparts and so are consequently more expensive, they still offer a shorter payback period [46]. Second-generation Kalina cycles therefore seem most promising, and configurations now exist for biomass, geothermal, solar thermal, cement waste heat, bottoming cycle, and ocean solar thermal applications [47].

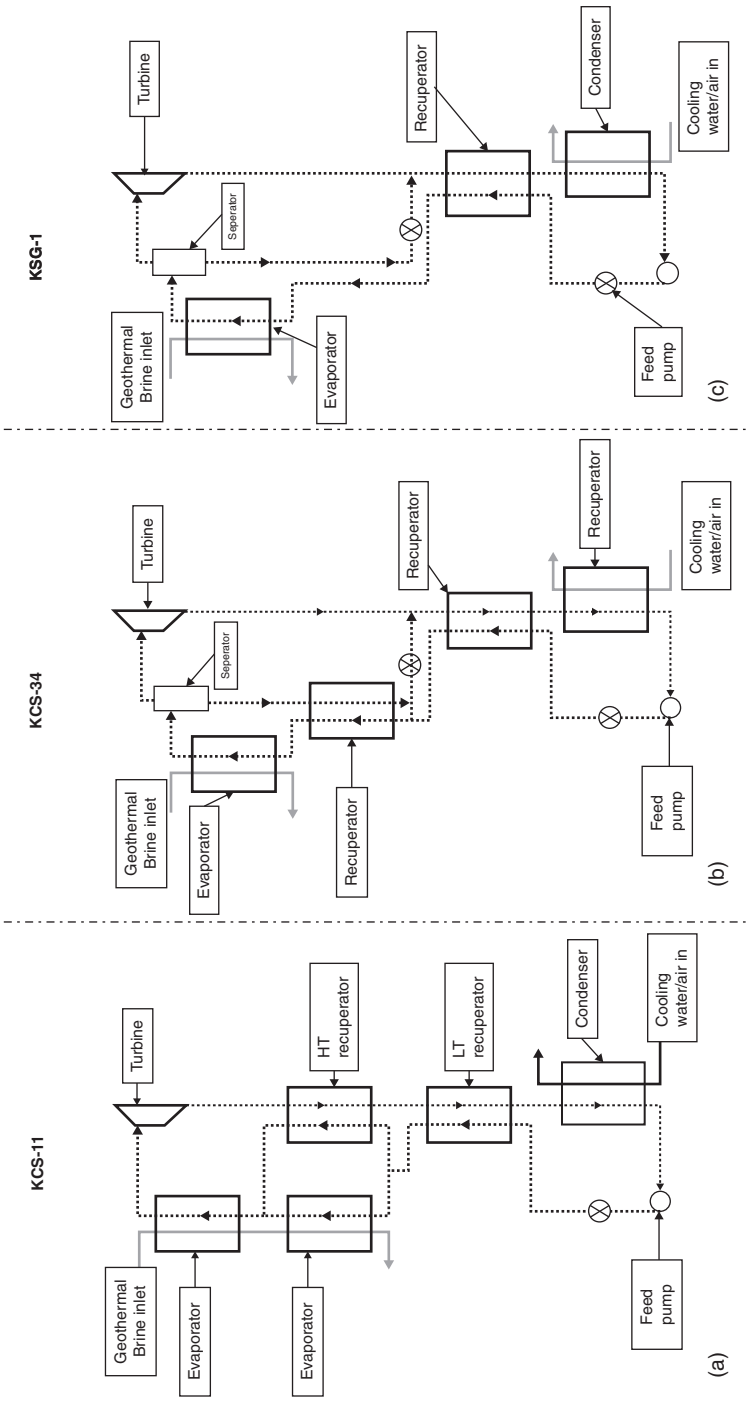

Figure 1.50 (a–c) Schematic of different Kalina cycle systems [44]. Source: Wang and Yu [44].

Table 1.4 Kalina cycle case studies from around the world [39].

Name	Country	Commissioned	Output (MW)	Heat sources
Canoga Park	USA	1992	6.5	Nuclear waste heat
Fukuoka	Japan	1998	4	Waste incineration
Sumitomo Metals	Japan	1999	3.5	Waste heat
Husavik	Iceland	2000	2	Geothermal
Fuji Oil	Japan	2005	3.9	Waste heat
Bruschal	Germany	2009	0.6	Geothermal
Unterhaching	Germany	2009	3.5	Geothermal
Shanghai Expo	China	2010	0.05	Solar hot water
Quingshui	Taiwan	2011	0.05	Geothermal

Source: Global cement [39].

1.4.4 Case Studies

Some pilot power plants exist and are currently producing energy using Kalina cycles. Table 1.4 lists case studies from around the world as of 2012.

The first large-scale Kalina cycle-based power plant was built in the United States in 1992 and operated for five years recovering nuclear waste heat and was able to produce 6.5 MW of electricity [39].

A famous Kalina-based plant (KCS-34) was built in Húsavík, Iceland. It is a 2 MW geothermal power plant and harnesses the energy of 125 °C geothermal brine, providing 80% of the electrical demand of the local town's 2500 inhabitants [48]. Another geothermal power plant (KCS34), also harnessing geothermal hot brine through a Kalina cycle, is located at Unterhachting in Germany. This power plant is generating 3.4 MW of electricity. The geothermal brine is also providing 38 MW of thermal energy to a district heating system. A third geothermal power plant (KCS-34) using the Kalina technology is the Bruchsal power plant [49], also in Germany.

Further Kalina cycle projects had been designed since 2012. For example, the Star Cement plant in Dubai is a 4.75 MW plant also using this technology [3], and it is anticipated, as we move forward, that more and more projects utilising Kalina cycles technology will evolve [50].

1.5 Brayton Cycle

The Brayton cycle is also known as the 'gas turbine cycle' or the *Joule* cycle. It is an open cycle, whereby the intake and exhaust points are both open to the environment [51].

Air enters the engine and is compressed by the compressor (resulting in HP air). Energy is then added by spraying fuel into the air and igniting it within the combustion chamber, and now this high-temperature pressurised gas is used to drive a turbine (mounted on the same shaft as the compressor) to produce work output. Finally, the combusted gases and any unused energy leaves through the exhaust and in doing so some of this unused energy can be recovered.

First though, the Brayton cycle itself. This consists of a compression stage (process 1–2) which takes place adiabatically followed by a second stage (process 2–3) – the heat addition process – which occurs isobarically. The third stage (process 3–4) is an expansion process which occurs adiabatically and the final stage (process 4–1), heat rejection, occurs isobarically, all as shown in Figure 1.51.

The Brayton cycle is different from the Otto and Diesel cycles in that the processes occur within an open system. Therefore, in order to determine the heat transfer and work for the process an open system and steady flow analysis are used.

The schematic of the open Brayton process is shown in Figure 1.52, however, to further define the process as a cycle we need to include the heat output as shown in Figure 1.53.

The thermal efficiency of the Brayton η_{th} cycle is given by the following equation:

$$\eta_{th} = \frac{W_{net}}{Q_{in}} = 1 - \frac{Q_{out}}{Q_{in}} \tag{1.69}$$

where W_{net} (kJ) is the net work output of the system, Q_{in} (kJ) is the heat input, and Q_{out} (kJ) is the heat output.

The conservation of mass then gives:

$$\dot{m}_{in} = \dot{m}_{out} \tag{1.70}$$

$$\dot{m}_2 = \dot{m}_3 = \dot{m} \tag{1.71}$$

where m_2 and m_3 are the mass flow rate of fluid leaving the compressor and the mass flow rate entering the turbine (kg/s), respectively.

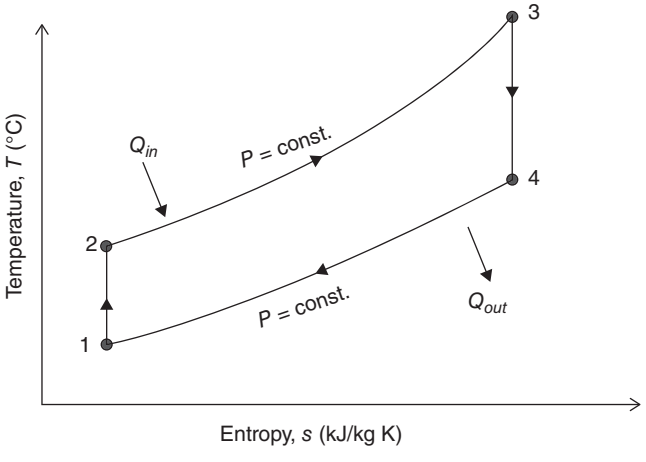

Figure 1.51 Temperature entropy graph for a Brayton cycle.

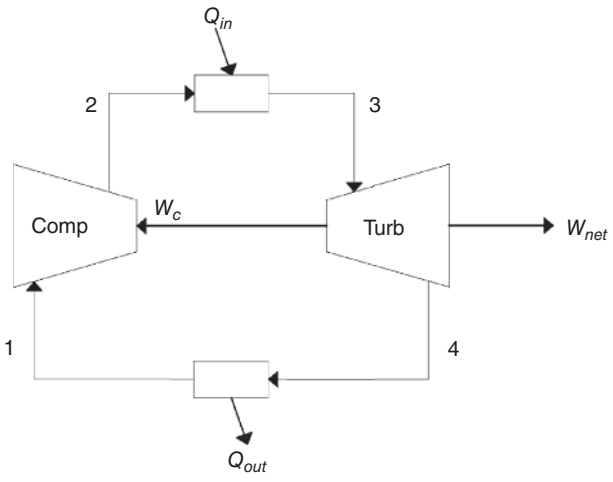

Figure 1.52 Gas turbine engine.

Figure 1.53 Closed Brayton cycle.

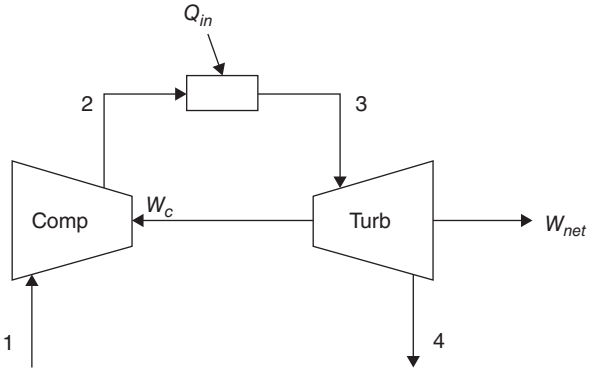

Therefore,

$$\eta_{th} = 1 - \frac{q_{out}}{q_{in}} = 1 - \frac{C_p(T_4 - T_1)}{C_p(T_3 - T_2)} \tag{1.72}$$

where $q_{out}(\text{kJ/kg}) = \frac{Q_{out}}{m}$, C_p (kJ/kg K) is the specific heat capacity of the working fluid (depending on the temperature), and T_x (K) is the temperature of the fluid given point.

Assuming the specific heat is constant (cold air standard analysis) gives:

$$\eta_{th} = 1 - \frac{T_4 - T_1}{T_3 - T_2} = 1 - \frac{T_1\left(\frac{T_4}{T_1} - 1\right)}{T_2\left(\frac{T_3}{T_2} - 1\right)} \tag{1.73}$$

And as processes 1–2 and 3–4 are isentropic:

$$\frac{T_2}{T_1} = \left(\frac{P_2}{P_1}\right)^{\frac{k-1}{k}} \tag{1.74}$$

$$\frac{T_3}{T_4} = \left(\frac{P_3}{P_4}\right)^{\frac{k-1}{k}} \tag{1.75}$$

In these last two equations, k is the heat capacity ratio, also known as the adiabatic index.

Moreover, as processes 2–3 and 4–1 are isobaric:

$$P_2 = P_3 \tag{1.76}$$

$$P_4 = P_1 \tag{1.77}$$

Thus,

$$\frac{T_2}{T_1} = \frac{T_3}{T_4} \tag{1.78}$$

Which can also be written this way:

$$\frac{T_4}{T_1} = \frac{T_3}{T_2} \tag{1.79}$$

So that finally, the efficiency of the ideal Brayton cycle is given by:

$$\eta_{th} = 1 - \frac{T_1}{T_2} \tag{1.80}$$

Now as the pressure ratio is defined as:

$$r_p = \frac{P_2}{P_1} \tag{1.81}$$

Figure 1.54 shows a typical pressure ratio curve for gas turbine engine.

Then the efficiency of the cycle can also be written using this coefficient as:

$$\eta_{th} = 1 - \frac{1}{r_p^{\frac{k-1}{k}}} \tag{1.82}$$

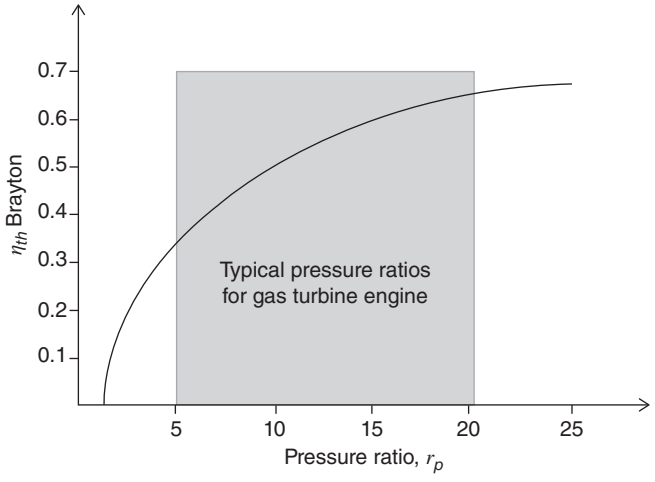

Figure 1.54 Typical pressure ratios for a gas turbine engine.

However, this is not the whole of the story because some of work produced by the turbine is also used by the compressor, the amount given back being defined by the back-work ratio (*BWR*) from:

$$BWR = \frac{W_{in}}{W_{out}} = \frac{W_{comp}}{W_{turb}} \tag{1.83}$$

1.5.1 Regenerative Brayton Cycle (Regenerator)

Because the temperature of the turbine exhaust is higher than the exit stream of the compressor, it presents an ideal opportunity to install a heat exchanger located between the hot exhaust of the turbine and the cooler gas leaving the compressor. Such a heat exchanger is also known as a regenerator or a recuperator. Figure 1.55 shows a schematic of the regenerative Brayton cycle.

And so in describing the efficiency of this regenerator, a *regenerator efficiency* term needs to be introduced, its calculation involving $q_{regen,max}$ and $q_{regen,act}$,and which can be obtained through enthalpy differences expressed in kJ/kg (see Figure 1.56).

$$\varepsilon_{regen} = \frac{q_{regen,max}\,(\text{kJ/kg})}{q_{regen,act}\,(\text{kJ/kg})} \tag{1.84}$$

$$q_{regen,max} = h_5' - h_2 = h_4 - h_2 \tag{1.85}$$

$$q_{regen,act} = h_5 - h_2 \tag{1.86}$$

Hence,

$$\varepsilon_{regen} = \frac{h_5 - h_2}{h_4 - h_2} \tag{1.87}$$

For ideal gases using the cold air standard analysis with constant specific heat, the regenerator effectiveness becomes:

$$\varepsilon_{regen} = \frac{T_5 - T_2}{T_4 - T_2} \tag{1.88}$$

So, for the efficiency of the cycle (using the closed cycle analysis) this leads to:

$$\eta_{th,regen} = 1 - \frac{q_{out}}{q_{in}} = 1 - \frac{h_6 - h_1}{h_3 - h_5} \tag{1.89}$$

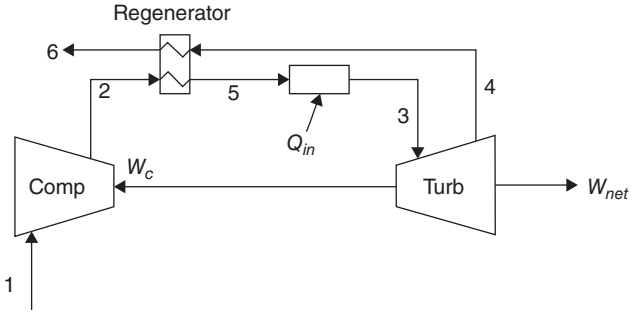

Figure 1.55 Schematic of the regenerative Brayton cycle.

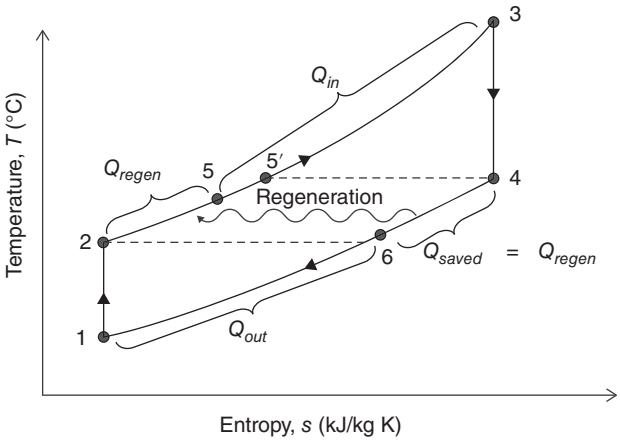

Figure 1.56 Temperature entropy graph for a regenerative Brayton cycle.

And assuming the efficiency of the regenerator is equal to 1, this then gives:

$$\eta_{th,regen} = 1 - \frac{T_1}{T_3} r_p^{\frac{k-1}{k}} \tag{1.90}$$

Figure 1.56 shows the temperature entropy profile for a regenerative Brayton cycle.

1.5.1.1 Compressor Analysis

The work (kW) used by the compressor is given by the following equation:

$$\dot{W}_{act,comp} = \dot{m}(h_{2a} - h_1) \tag{1.91}$$

where $\dot{m}$ is the mass flow rate of working fluid (in kg/s) and h_x is the enthalpy at the given point (kJ/kg).

Hence the adiabatic efficiency of the compressor is given by:

$$\eta_{comp} = \frac{\dot{W}_{isen,comp}}{\dot{W}_{act,comp}} = \frac{h_{2s} - h_1}{h_{2a} - h_1} \cong \frac{T_{2s} - T_1}{T_{2a} - T_1} \tag{1.92}$$

And the isentropic temperature at the outlet of the compressor is given by:

$$T_{2s} = T_1 \left(\frac{P_2}{P_1} \right)^{\frac{k-1}{k}} \tag{1.93}$$

1.5.1.2 Turbine Analysis

The work provided by the turbine (kW) is given by the following equation:

$$\dot{W}_{act,turb} = \dot{m}(h_3 - h_{4a}) \tag{1.94}$$

From which, the adiabatic efficiency of the turbine is given by:

$$\eta_{turb} = \frac{\dot{W}_{act,turb}}{\dot{W}_{isen,turb}} = \frac{h_3 - h_{4a}}{h_3 - h_{4s}} \cong \frac{T_3 - T_{4a}}{T_3 - T_{4s}} \tag{1.95}$$

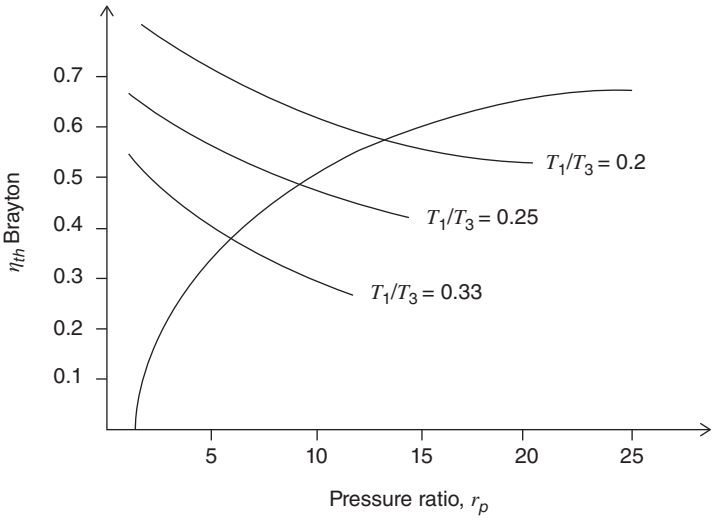

Figure 1.57 Regenerative Brayton cycle efficiency as a function of the pressure ratio and minimum and maximum temperature ratio.

And so, the isentropic temperature at the outlet of the turbine is given by:

$$T_{4s} = T_3\left(\frac{P_4}{P_3}\right)^{\frac{k-1}{k}} \tag{1.96}$$

1.5.1.3 Heat Supplied to the Cycle

The heat supplied to the cycle (kJ/kg) for process 5 to 3 can be calculated as follows:

$$q_{in} = h_3 - h_5 = C_p(T_3 - T_5) \tag{1.97}$$

The plot in Figure 1.57 shows the regenerative Brayton cycle efficiency as a function of the pressure ratio and minimum and maximum temperature ratio, T_1/T_3.

Thus, when the efficiency of the regenerative cycle is equal to the standard Brayton cycle then:

$$r_p = \left(\frac{T_3}{T_1}\right)^{\frac{k}{2(k-1)}} \tag{1.98}$$

1.5.2 Regenerative Brayton Cycle (Reheater and Intercooler)

The performance of a Brayton cycle can be further improved by incorporating an intercooler and a reheat process, the process schematic in Figure 1.58 shows a potential layout for a Brayton cycle with such additions. The concept is simple. During multi-stage compression, cooling the working fluid between each stage ultimately reduces the amount of work that is required by each compressor. This is because if we reduce the specific volume of the working fluid by cooling, then less work is required to achieve a set pressure increase.

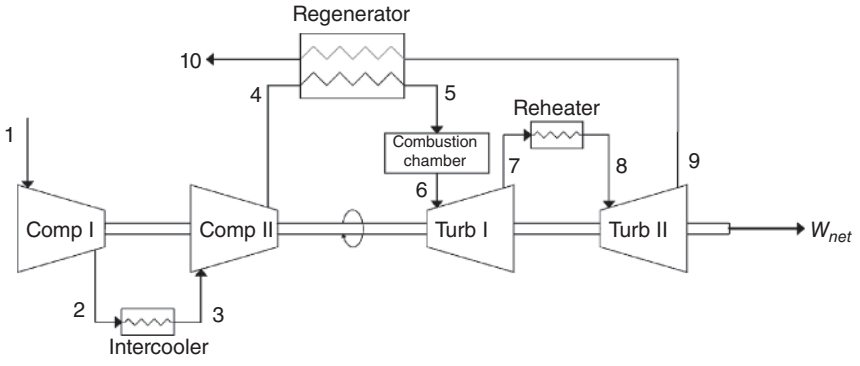

Figure 1.58 Schematic of the regenerative Brayton cycle with intercooler and reheat.

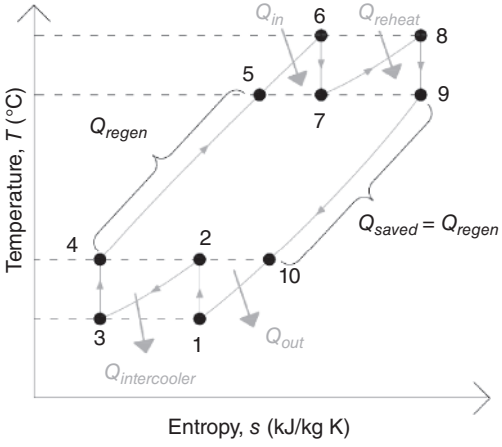

Figure 1.59 Temperature entropy graph for a regenerative Brayton cycle with a reheater and an intercooler.

So, incorporating a reheating process between two or more turbines of a multi-stage expansion ultimately results in an increase in the net work done and therefore a more efficient cycle. The temperature against entropy for this thermodynamic cycle is shown in Figure 1.59.

1.5.2.1 Intercooling

To minimise the work used by the compressors, P_2 (Pa) should be set as:

$$P_2 = \sqrt{P_1 P_4} \tag{1.99}$$

As the process 2–3 is isobaric, it can also be written as follows:

$$\frac{P_2}{P_1} = \frac{P_4}{P_2} = \frac{P_4}{P_3} \tag{1.100}$$

1.5.2.2 Reheating

To maximise the turbine work, P_7 should be set as:

$$P_7 = \sqrt{P_6 P_9} \tag{1.101}$$

As the process 7–8 is isobaric, it can also be written this way:

$$\frac{P_6}{P_7} = \frac{P_7}{P_9} = \frac{P_8}{P_9} \tag{1.102}$$

1.6 Chapter Summary

To conclude, the Rankine cycle can be considered (alongside the Carnot cycle) as the basis for all the external combustion thermodynamic cycles that aim to convert thermal energy into mechanical energy. In most cases the mechanical energy is then converted into electrical energy because of its greater versatility and adaptability as a form of energy.

Even though the ideal Rankine cycle is quite simple, a significant number of improvements can still be made to it in order to enhance the performance of the system and increase its energetic efficiency – reheating, regeneration, increasing or decreasing the pressure can all be considered, in order to make the most of a power plant.

In most cases, water is used as the working fluid because it is non-toxic, non-reactive, abundant, cost-effective, and displays good thermodynamic properties. However, using an organic fluid is also an option to help further increase the efficiency of the Rankine cycle or to harness medium temperature hot sources such as geothermal, biomass solar energy, or for waste heat recovery. In which case, this new cycle is known as an ORC, but even this can be further improved in many ways using reheaters and/or recuperators for instance. The use of new fluids also allows for greater flexibility, in that different fluids may be more suitable for specific applications, thus allowing them to reach their greatest possible efficiency. Hence, as discussed earlier, the selection of the right working fluid is crucial to efficient operation. To assist in this choice, organic fluids are divided into three families: wet-type fluids, dry-type fluids, and isentropic fluids, and currently a huge number of studies are focusing on the integration of ORC with existing systems so as to improve their overall efficiency.

Recent technological advances also allow the working fluid (water or organic fluid) to be used in supercritical conditions in order to improve the amount of work provided by the turbine(s) of a power plant.

In this respect, the Kalina cycle can be considered as the biggest step forward since the development of the Rankine steam cycles and ORCs. The technology presents a better energetic efficiency than steam cycles particularly for low-grade temperature applications such as geothermal and waste heat recovery.

The technology is relatively new; hence the capital expenditure necessary for a Kalina cycle-based power plant is, in most cases, higher than for a conventional system. However, as the Kalina cycle systems have a higher efficiency, their payback period is reduced, particularly for the latest second-generation cycles. It is also important to note that the Kalina cycles are a family of thermodynamic cycles and so a vast number of configurations exist, each one being suitable for a specific application. In most cases, a water–ammonia mixture is used as the working fluid in those

employing binary cycles. Indeed, this fluid offers interesting thermal performance; is compatible with standard materials and components; is ecological-friendly, abundant, and relatively inexpensive.

The reverse Kalina cycle is also a widely known thermodynamic cycle in that it is the absorption refrigeration cycle. This cycle uses an absorber and a generator instead of a compressor to carry out the suction and compression processes, meaning that almost no electricity is required to run the cycle. The future of Kalina cycles seems promising. An ever-increasing number of scientific studies are addressing the integration of this cycle in various systems: geothermal power plants, cement plants, concentrated solar power plants, and biomass power plants.

Now the Brayton cycle, although different to the Rankine cycle and its derivatives in that it is an open thermodynamic cycle, still has the same role to play as the closed power cycle – converting heat into mechanical energy – and the cycle efficiency can also be improved by using different technologies such as regeneration, reheating, and intercooling. The Brayton cycle can also use organic fluids as their working fluid (CO_2 in most cases) and sometimes these fluids too can operate under supercritical conditions with a further increase in efficiency.

But we are not just thinking about systems in isolation. Even if Rankine cycles and Brayton cycles are quite different, they can still be used together in combined cycles. In the CCGT plant, those two cycles are used together to reach a relatively high overall thermal efficiency (from 50% to 63%). So high, that the association of the Rankine cycle with the Brayton cycle is currently the most efficient way of producing electricity on a large scale. For example, the Chubu Electric Nishi-Nagoya power plant Block-1 in Japan is achieving a gross efficiency of 63.08%, and so is currently recognised as the world's most efficient combined cycle power plant.

References

1 Zhou, F., Joshi, S.N., Rhote-Vaney, R., and Dede, E.M. (2017). A review and future application of Rankine cycle to passenger vehicles for waste heat recovery. *Renewable Sustainable Energy Rev.* 75: 1008–1021. https://doi.org/10.1016/j.rser.2016.11.080.

2 Sattari, A. (2017). A novel design of a low Cost CSP using turbocharger as an expander. *J. Sol. Energy Res.* 2: 20–24.

3 Janie Ling-Chin, H.B.Z.M., Taylor, W., and Roskilly, A.P. (2019). Chapter 4: State-of-the-art technologies on low-grade heat recovery and utilization in industry. In: *Energy Conversion. Current Technologies and Future Trends*. IntechOpen https://doi.org/10.5772/intechopen.78701.

4 Sethi, A., Vera Becerra, E., and Yana Motta, S. (2016). Low GWP R134a replacements for small refrigeration (plug-in) applications. *Int. J. Refrig.* 66: 64–72. https://doi.org/10.1016/j.ijrefrig.2016.02.005.

5 Shang, R., Zhang, Y., Shi, W. et al. (2014). Fresh look and understanding on carnot cycle. *Energy Procedia* 61: 2898–2901. https://doi.org/10.1016/j.egypro.2014.12.213.

6 Xu, W., Deng, S., Su, W. et al. (2018). How to approach Carnot cycle via zeotropic working fluid: Research methodology and case study. *Energy* 144: 576–586. https://doi.org/10.1016/j.energy.2017.12.041.

7 Greitzer, E.M. (n.d.). 8.6 Enhancements of Rankine cycles.ZSSI.

8 Weston, K.C. (2000). *Fundamentals of Steam Power 2.1 Introduction*, 1e. University of Tulsa.

9 Riddoch, F. and Craenen, S. (n.d.). Cogeneration at the foundation of Europe's energy policy.

10 IBGE. (n.d.). Guide Cogénération.

11 Mat, N., Chee, I., Tan, W., and Yatim, A.H.M. (2018). A comprehensive review of cogeneration system in a microgrid: a perspective from architecture and operating system. *Renewable and Sustainable Energy Rev.* 81 (Part 2): 2236–2263. https://doi.org/10.1016/j.rser.2017.06.034.

12 Dabwan, Y.N. and Pei, G. (2020). A novel integrated solar gas turbine trigeneration system for production of power, heat and cooling: thermodynamic-economic-environmental analysis. *Renewable Energy* 152: 925–941. https://doi.org/10.1016/j.renene.2020.01.088.

13 Goncalv, E., Silva, D., Thibault, J. (2008). Cycles thermodynamiques des machines thermiques. Institut Polytechnique de Grenoble, 153.

14 Association WN. (n.d.). Advanced Nuclear Power Reactors | Generation III+ Nuclear Reactors.

15 Administration USEI. (n.d.). SAS Output.

16 Quoilin, S., Van Den, B.M., Declaye, S. et al. (2013). Techno-economic survey of organic rankine cycle (ORC) systems. *Renewable Sustainable Energy Rev.* 22: 168–186. https://doi.org/10.1016/j.rser.2013.01.028.

17 Al-Taha WH, Osman HA. Performance analysis of a steam power plant: a case study 2018. MATEC Web of Conferences, Volume 225, UPT-UMP-VIT Symposium on Energy Systems doi:https://doi.org/10.1051/matecconf/201822505023.

18 Inc AP. (n.d.). Economics and feasibility of rankine cycle improvements for coal fired power plants.

19 Minea, V. (2014). Power generation with ORC machines using low-grade waste heat or renewable energy. *Appl. Therm. Eng.* 69: 143–154. https://doi.org/10.1016/j.applthermaleng.2014.04.054.

20 Darvish, K., Aliehyaei, M., Atabi, F., and Rosen, M. (2015). Selection of optimum working fluid for organic Rankine cycles by exergy and exergy-economic analyses. *Sustainability* 7: 15362–15383. https://doi.org/10.3390/su71115362.

21 Abas, N., Kalair, A.R., Khan, N. et al. (2018). Natural and synthetic refrigerants, global warming: a review. *Renewable Sustainable Energy Rev.* 90: 557–569. https://doi.org/10.1016/j.rser.2018.03.099.

22 Nair, V. (2021). HFO refrigerants: a review of present status and future prospects. *Int. J. Refrig.* 122: 156–170. https://doi.org/10.1016/j.ijrefrig.2020.10.039.

23 Linde Group (2013). Safety Data Sheet – Heptafluorpropane (R227).

24 Linde Group (2014). Safety Data Sheet – Pentafluoropropane (R245fa).

25 Linde Group (2013). Safety Data Sheet – Isobutane (R600a).

26 Yang, H., Xu, C., Yang, B. et al. (2020). Performance analysis of an organic Rankine cycle system using evaporative condenser for sewage heat recovery in the petrochemical industry. *Energy Convers. Manage.* 205: 112402. https://doi.org/10.1016/j.enconman.2019.112402.

27 Baldasso, E., Andreasen, J.G., Mondejar, M.E. et al. (2019). Technical and economic feasibility of organic Rankine cycle-based waste heat recovery systems on feeder ships: impact of nitrogen oxides emission abatement technologies. *Energy Convers. Manage.* 183: 577–589. https://doi.org/10.1016/j.enconman.2018.12.114.

28 Yue, C., Tong, L., and Zhang, S. (2019). Thermal and economic analysis on vehicle energy supplying system based on waste heat recovery organic Rankine cycle. *Appl. Energy* 248: 241–255. https://doi.org/10.1016/j.apenergy.2019.04.081.

29 Sikarwar, S.S., Surywanshi, G.D., Patnaikuni, V.S. et al. (2020). Chemical looping combustion integrated organic Rankine cycled biomass-fired power plant – Energy and exergy analyses. *Renewable Energy* 155: 931–949. https://doi.org/10.1016/j.renene.2020.03.114.

30 Alvi, J.Z., Feng, Y., Wang, Q. et al. (2020). Modelling, simulation and comparison of phase change material storage based direct and indirect solar organic Rankine cycle systems. *Appl. Therm. Eng.* 170: 114780. https://doi.org/10.1016/j.applthermaleng.2019.114780.

31 Li, W., Lin, X., Cao, C. et al. (2018). Organic Rankine cycle-assisted ground source heat pump combisystem for space heating in cold regions. *Energy Convers. Manage.* 165: 195–205. https://doi.org/10.1016/j.enconman.2018.03.062.

32 Saghafifar, M., Omar, A., Mohammadi, K. et al. (2018). A review of unconventional bottoming cycles for waste heat recovery: Part I-Analysis, design, and optimization. *Energy Convers. Manag.* 198 https://doi.org/10.1016/j.enconman.2018.10.047.

33 Zhang, X., He, M., and Zhang, Y. (n.d.). A review of research on the Kalina cycle. *Renewable Sustainable Energy Rev.* 16 (7) https://doi.org/10.1016/j.rser.2012.05.040.

34 Globalgeothermal. (n.d.) Global Geothermal-Kalina Cycle application.

35 Schenker, S., Mccandless, D.W., Brophy, E., and Lewis, M.S. (1967). Studies on the intracerebral toxicity of ammonia. *J. Clin. Investig.* 46: 838–848.

36 Ambriz-Díaz, V.M., Rubio-Maya, C., Chávez, O. et al. (2021). Thermodynamic performance and economic feasibility of Kalina, Goswami and Organic Rankine Cycles coupled to a polygeneration plant using geothermal energy of low-grade temperature. *Energy Convers. Manag.* 243: 114362. https://doi.org/10.1016/j.enconman.2021.114362.

37 Global cement. (n.d.). Kalina bottoming cycle vs Rankine (ORC) in thermal power plant design.

38 Mirolli, M., Happ, K. (2012). Global CempPower Conference. FLSmidth & Co A/S.

39 Global cement. (2012). Kalina Cycle power systems in waste heat recovery applications.

40 Omar, A., Saghafifar, M., Mohammadi, K. et al. (2018). A review of unconventional bottoming cycles for waste heat recovery: Part II-Applications. *Energy Convers. Manage.* https://doi.org/10.1016/j.enconman.2018.10.088.

41 Kalinapower. (n.d.). Kalina – Electricity from heat.

42 Blanco, M. and Lourdes, R.S. (2017). *Advances in Concentrating Solar Thermal Research and Technology*. Google Livres.

43 Nasruddin, U.R., Rifaldi, M., and Noor, A. (2009). Energy and exergy analysis of kalina cycle system (KCS) 34 with mass fraction ammonia-water mixture variation. *J. Mech. Sci. Technol.* 23: 1871–1876. https://doi.org/10.1007/s12206-009-0617-8.

44 Wang, E. and Yu, Z. (2016). A numerical analysis of a composition-adjustable Kalina cycle power plant for power generation from low-temperature geothermal sources. *Appl. Energy* 180: 834–848. https://doi.org/10.1016/j.apenergy.2016.08.032.

45 Kalex Systems LLC. (2009). Kalex Kalina Cycle Power Systems for Geothermal Applications.

46 Renz, M., Engelhard, M., Zander, M. (2006). The New Generation Kalina Cycle Contribution to the conference "*Electricity Generation from Enhanced Geothermal Systems*."

47 Kalex Systems LLC. (2009). Kalex Kalina Cycle Power Systems for Geothermal Applications.

48 Lcak HM, Ark M, Irolli M, Hjartarson H, Húsavíkur O. (2002). Notes from the North: A Report on the Debut Year of the 2 MW Kalina Cycle ® Geothermal Power Plant in Húsavík, Iceland.

49 G-u M. (2010). *The Geothermal Power Plant Bruchsal*.

50 Kalina Power. (2016). Introduction to Kalina Cycle®. Kalina Power Limited.

51 Huang, K., Marthinsen, K., Zhao, Q., and Logé, R. (2018). The double-edge effect of second-phase particles on the recrystallization behaviour and associated mechanical properties of metallic materials. *Prog. Mater. Sci.* 92: 284–359. https://doi.org/10.1016/j.pmatsci.2017.10.004.